the substrate solution, 120 μl of 0.1 mg/ml 3,3′,5,5′-tetramethylbenzidine (Dojindo, Kumamoto, Japan) solution in *N,N*,dimethylformamide and 1.3 μl of 30% H_2O_2 was mixed with 7.88 ml of 0.1 M sodium acetate buffer, pH 5.5, immediately before use. A 0.5 μg amount of ssDNA or dsDNA dissolved in 50 μl of PBS were allowed to dry in a flat 96-well NUNC-IMMUNO Plate (Nunc, Roskilde, Denmark). Wells were blocked with 3% BSA in PBS and washed with PBS-Tween. A 50 μl of the serum (diluted to 1:100) was added to a well in triplicate, and allowed to stand at room temperature for 2 h. After five washes with PBS-Tween, HRP-conjugated donkey anti-mouse μ chain antibodies or rabbit anti-mouse γ chain antibodies (Jackson Laboratory; diluted to 1:2,000) in 1% BSA in PBS was added to each well and incubated for 1 h at room temperature. After three washes with PBS-Tween, 50 μl of substrate solution was added, and the plates were incubated at room temperature until the solution turned yellow. The reaction was stopped by adding 50 μl of 2 M H_2SO_4, and absorbance at 450 nm was measured with a microplate reader (Model 550 Bio-Rad, Richmond, CA).

Results and discussion

The antisera obtained from Balb/c mice in response to subcutaneous injection of rafts prepared from a variety of cell lines were examined by TLC-immunostaining to analyze the reactivity of the antibodies against glycolipids. Both ACHN cells and Vero cells are derived from kidney and express globoseries glycosphingolipids whereas Karpas cells predominantly express LacCer, and EL4 cells mainly express GM2 and GD2 (Fig. 1a). The antisera obtained by injection with ACHN rafts and Vero rafts were found to uniquely bound to sialylGb5, suggesting the development of mono-specific antibodies against sialylGb5 (Fig. 1b). As we previously showed, ACHN cells contain comparable amounts of Gb3, Gb4, Gb5, and sialyGb5, suggesting that the sialylGb5 of ACHN cells is strongly immunogenic [2]. The antisera obtained by injection with Karpas rafts were also found to specifically bind to a single glycolipid that has not yet been identified. Since the glycolipid was stained with resorcinol and not bound by choleratoxin even after digestion with *Clostridium perfringens* sialidase (data not shown), it is suggested that this antigen is a sialylated non-ganglioseries glycolipid. The observation that the anti-Karpas rafts antisera did not bind to any glycolipid extracted from mouse brains in which various kinds of gangliosides are abundantly contained (data not shown) should support this idea. The antisera obtained by injection with EL4 rafts were found to uniquely react with GD2. However, when antisera obtained by injection of rafts prepared from the other cell lines, *i.e.*, B16F1, P3U1, RL-2, Molt 4, Jurkat, or NALM-6, were tested, no such monoglycolipid-specific reactivity was observed (data not shown). These findings indicate that immunization with rafts prepared from some specific cell lines can induce the development of monoglycolipid-specific antibodies. Since we obtained identical results in a similar experiment in C57BL/6 mice (Fig. 1c), the development of monoglycolipid-specific antibodies is a common feature of immunization of these cell lines with rafts and not a phenomenon specific to a certain strain of mice.

Immunization of mice with a suspension of whole cells is one of the ways that is often used to obtain monoclonal antibodies against cell surface molecules [6, 7]. We therefore investigated whether whole-cell immunization is capable of inducing the development of monoglycolipid-specific antibodies in mice, the same as raft immunization does. The antisera obtained by injection with Vero, Karpas, and EL4 cell suspensions did not react with certain specific glycolipids, and only the antisera obtained by immunization with ACHN cell suspensions yielded a mono-specific reaction with sialylGb5 (Fig. 2). This suggests that immunization with suspensions of whole cells does not usually induce the development of monoglycolipid-specific antibodies and that the rafts on the cell surface of ACHN cells assemble in a manner that is favorable for inducing immune reactions against sialylGb5.

Next, we examined the quantitative and qualitative kinetics of the production of the specific antibodies in sera by immunization with rafts derived from ACHN cells. The antisera obtained after each immunization were examined by dot-blot immunostaining and TLC immunostaining (Fig. 3a). The relative amounts of antibodies that bound to rafts dot-blotted on a PVDF membrane or lipids separated on a TLC plate were shown as PSL (Fig. 3b). Production of IgM class anti-raft antibodies was detected after the second immunization, and it peaked after the third immunization, and then decreased. Production of IgG class anti-raft antibodies was also detected after the second immunization, but at a low level, and it continued to increase even after the fourth immunization. The specificity of the secondary antibodies used for typing the immunoglobulin class of anti-raft antibodies was confirmed in advance (data not shown). No anti-sialylGb5 antibodies were detected not after the first immunization (data not shown). They were faintly detected after the second immunization, and then increased in an immunization time-dependent manner. These results indicate that the production of anti-raft antibodies in mice is a typical immune response accompanying the class switch from IgM antibodies to IgG antibodies. Interestingly, the #3 antisera of the third immunization gave strong reactivity with the lower band glycolipid, while that of the fourth

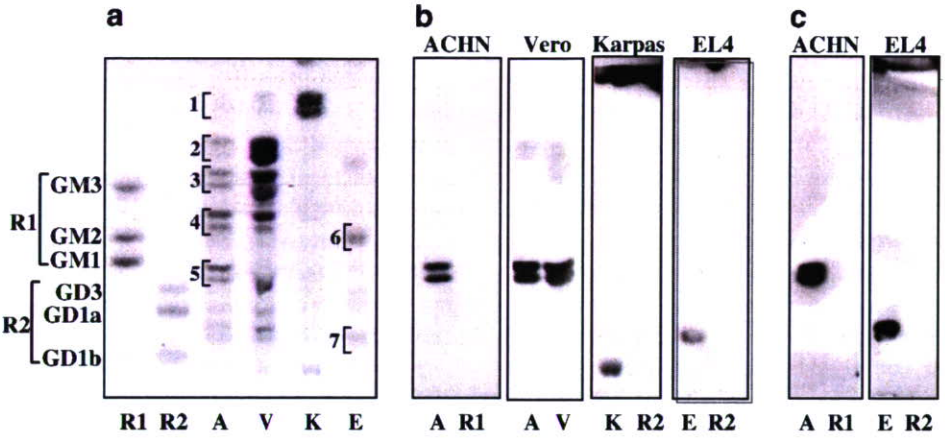

Fig. 1 TLC immunostaining with antisera against rafts components. The lipids extracted from ACHN (*A*), Vero (*V*), Karpas (*K*), EL4 (*E*) cells and the reference glycolipids (*R1* GM3, GM2, GM1; *R2* GD3, GD1a, GD1b) were separated by TLC and chemically stained with Orcinol reagent (**a**) or immunostained with antisera of Balb/c mice (**b**) and C57BL/6 mice (**c**) that had been immunized with rafts prepared from ACHN cells, Vero cells, Karpas cells and EL4 cells. Lipids extracted from 5×10^6 cells and 1×10^6 cells of each cell line are subjected to TLC for Orcinol staining and immunostaining, respectively. *1* LacCer; *2* Gb3; *3* Gb4; *4* Gb5; *5* sialylGb5; *6* GM2; *7* GD2

immunization reacted strongly with the upper band glycolipid (Fig. 3a). The result may indicate that ceramide structure is also involved in antigen presentation of glycolipid in rafts.

Next, we examined the correlation between the amounts of rafts injected and anti-raft antibody production. To do so, we immunized C57BL/6 mice with rafts prepared from various numbers of EL4 cells and evaluated the subsequent production of anti-EL4 raft antibodies by flow cytometry and TLC immunostaining. As shown in Fig. 4a, the amounts of anti-EL4 raft antibody increased with the amounts of EL4 rafts injected. Injection with the rafts prepared from 0.12×10^7 EL4 cells induced a slight elevation of reactivity, and the rafts prepared from 3×10^7 EL4 cells were sufficient to induce maximum reactivity. Rafts prepared from more than 0.6×10^7 EL4 cells appeared to be needed to obtain a significant level of anti-GD2 antibodies, (Fig. 4b).

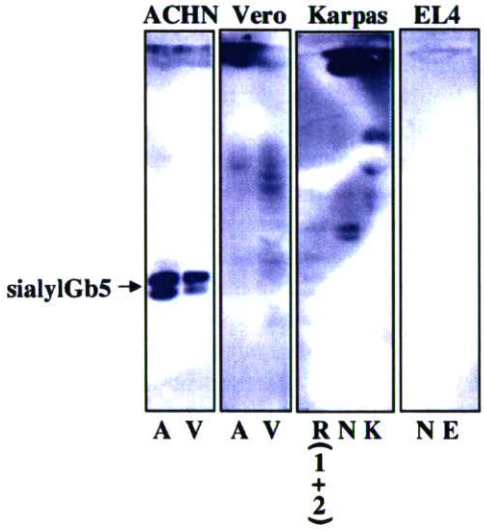

Fig. 2 TLC immunostaining with antisera against the cell suspension. The lipids were extracted from the cells as shown in the legends to Fig. 1 and from NALM-6 cells (*N*), and separated by TLC. The plates were immunostained with antisera from Balb/c mice immunized with the suspension of irradiated ACHN cells, Vero cells, Karpas cells, and EL4 cells

Since EL4 cells are derived from C57BL/6 mice, no immune responses to EL4 cells or EL4 cell components should be usually induced in syngeneic C57BL/6 mice. However, the injection of C57BL/6 mice with the EL4 rafts resulted in production of anti-raft antibodies in syngeneic mice as shown above. We therefore tried using flow cytometry to corroborate that injection of raft suspensions can induce anti-raft antibody production in syngeneic mice. The results showed that the antisera of C57BL/6 mice injected with rafts of syngeneic melanoma cell line B16F1 bound to B16F1 cells (Fig. 5a). Both mouse myeloma cell line P3U1 and lymphoma cell line RL-2 are derived from Balb/c mice, and antisera from Balb/c mice injected with rafts of these syngeneic P3U1 (Fig. 5b) and RL-2 rafts (Fig. 5c) were also confirmed to bind to P3U1 cells and RL-2 cells, respectively. Injection of mice with a PBS suspension of irradiated syngeneic cells did not result in the production of antisera that bound to syngeneic cells (data not shown).

Since repeated immunization of self- or syngeneic antigens is thought to induce autoimmune diseases, we repeated injection of C57BL/6 mice with EL4 rafts or Balb/c mice with the P3U1 rafts and investigated whether the mice produced anti-DNA antibodies by ELISA. The average A_{450} of anti-ssDNA IgM in the sera of the mice injected with PBS and the syngeneic rafts was 0.247±0.027

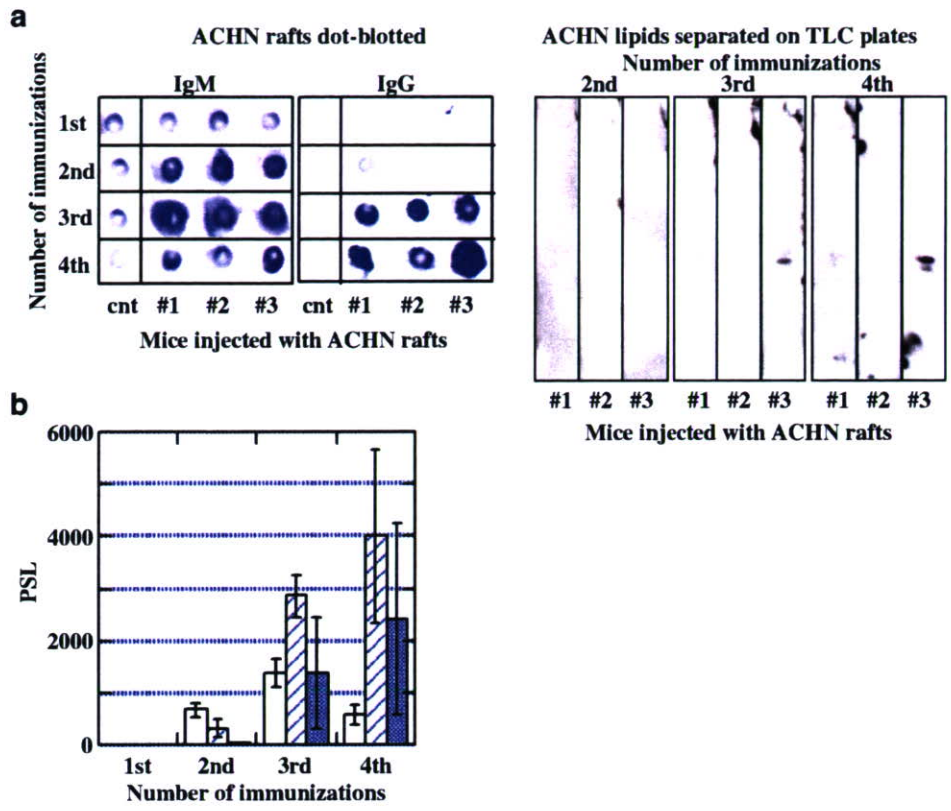

Fig. 3 Kinetics of production of antibody against ACHN rafts. Balb/c mice were injected with an ACHN raft suspension in triplicate (*#1*, *#2*, *#3*) or PBS (*cnt*) four times at 7 day intervals, and the sera were obtained 5 days after each immunization. The rafts dot-blotted on PVDF membranes were probed with each antiserum, and then probed with the HRP-conjugated anti-mouse IgM μ chain-specific antibodies or IgG γ chain-specific antibodies as secondary antibody. The lipids separated on the TLC plate were probed with each antiserum, and then with the HRP-conjugated anti-mouse IgG+M antibodies. **a** The images of dot-blot immunostaining of ACHN rafts (*left*) and TLC immunostaining of ACHN lipids (*right*) with the antisera. **b** Measurement of anti-raft IgM antibodies (*open column*), the anti-raft IgG antibodies (*striped column*), and anti-sialylGb5 antibodies (*shaded column*)

(column 1 in Fig. 6) and 0.240±0.043 (column 2 in Fig. 6), respectively, and the difference between the two groups was not significant. The A_{450} for anti-ssDNA IgM in the serum of NZB/WF1, which are well known to spontaneously develop autoimmune disease, was 0.325. No elevation of IgG class anti-DNA antibodies or anti-dsDNA antibodies was observed in the sera of either the immunized mice or NZB/WF1 mice (data not shown). No anti-DNA antibody production or other diagnostic signs of autoimmune disease were observed in these mice. These results show that the development of antibodies against syngeneic rafts components by the mice was not due to the development of an autoimmune disease.

The results of this study show that subcutaneous injection of mice with rafts prepared from specific cell lines induces production of antibodies that recognize single glycolipids, namely monoglycolipid-specific antibodies. For example, rafts prepared from ACHN cells and Vero

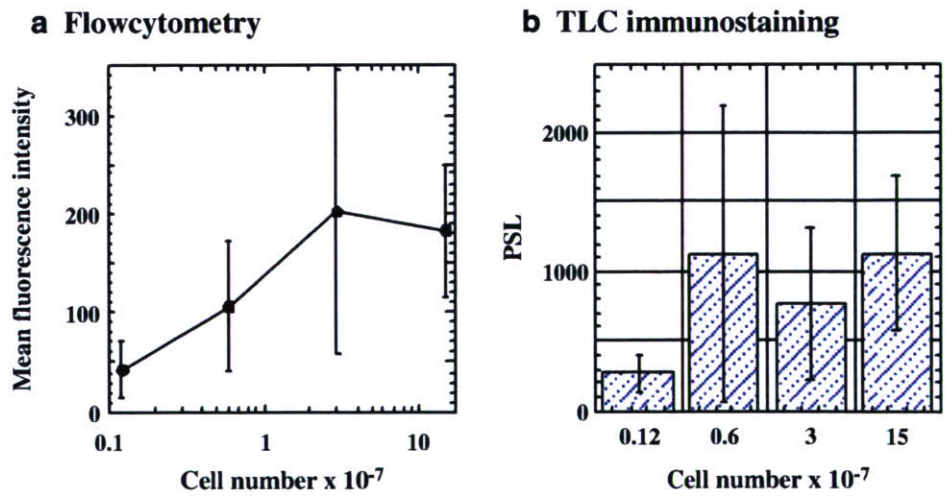

Fig. 4 Reactivity of mouse sera after immunization with the rafts prepared from various numbers of EL4 cells. The sera were obtained from C57BL/6 mice immunized with rafts prepared from 0.12, 0.6, 3 and 15×10^7 EL4 cells. The experiments were performed in triplicate. **a** Evaluation of antibody reactivity to EL4 cells by flowcytometry. **b** Evaluation of antibody reactivity to GD2 by TLC immunostaining

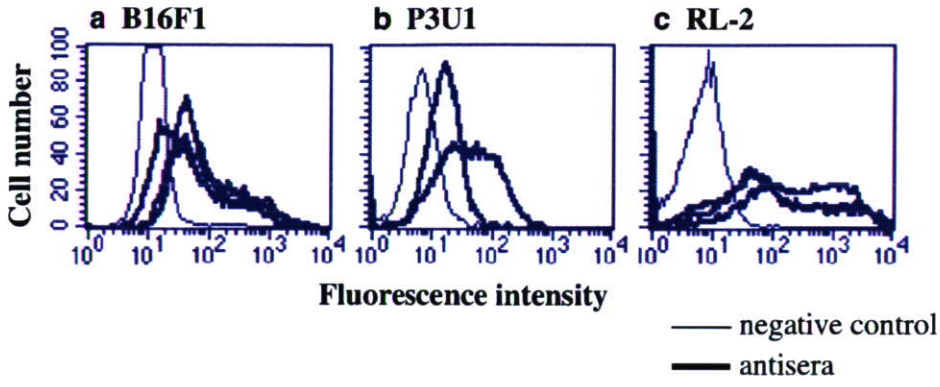

Fig. 5 Flow cytometric analysis of the antisera of mice immunized with syngeneic rafts. Cells were stained with the antisera of C57BL/6 mice immunized with B16F1 rafts (**a**), Balb/c mice immunized with P3U1 rafts (**b**) and Balb/c mice immunized with RL-2 rafts (**c**), and analyzed by flow cytometry (*bold line*). The sera of each mouse injected with PBS were used as a negative control (*thin line*)

cells strongly induced the production of mono-specific antibodies against sialyGb5. However, since sialyGb5 is not the quantitatively predominant glycolipid in ACHN cells or Vero cells, quantitative lipid dominance may not be necessary for monospecific antibody production. Since all four glycolipids to which specific antibodies were produced shown in Fig. 1b were sialylated, sialylation is thought to be the most important factor for inducing monospecific antibody production. However, the rafts from other cell lines gave no production of such antibodies. For example, although B16 melanoma cells are known to highly express GM3 [8], injection of the B16 melanoma rafts did not induce monoglycolipid-specfic antibody. Since Kawashima *et al.* [9] reported that when they intravenously injected ten strains of inbred mice with 100 μg of gangliosides adsorbed to *Salmonella minnesota*, gangliosides such as GD3, GD2, GD1b, GT1a, and GQ1b that have a trisaccharide sequence of NeuAcα2,8NeuAα2,3Gal induced high-titer antibody responses, whereas gangliosides such as GM4, GM3, GM2, GM1, GD1a, and GT1b that have a disaccharide sequence of NeuAcα2,3Gal induced low-titer antibody responses, the diversity of immunogenicity among the glycolipids should be present. Since SSEA-4, an epitope carried by sialyGb5 has been well known highly immunogenic, a saccharide sequence of sailylGb5 can be thought to induce high-titer antibody production. Therefore, if the cells contain highly immunogenic glycolipids such as sialyGb5 and GD2 in lipid rafts, these glycolipids may be effectively presented as immunological targets for antibody production, whereas the rafts containing only low immunogenic glycolipids may be insufficient for antigen presentation to produce anti-glycolipids antibodies. Yamazaki Y. *et al.* [10] obtained several monoclonal antibodies by injecting mice with HL60 cell lipid rafts. One of the antibodies reacted with both GM1a and GD1b, and another reacted with phosphatidylglucoside. HL60 cells, however, mainly express glycolipids of the neolactoseries, not the ganglioseries [11], suggesting that raft immunization enables antibody production against such an extremely minor glycolipid. In order to induce effective

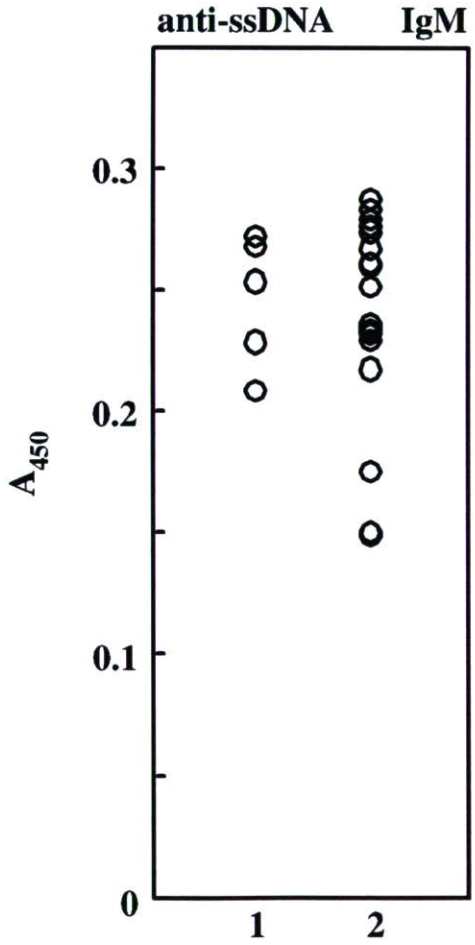

Fig. 6 ELISA of anti-ssDNA antibodies in the sera of mice immunized with syngeneic rafts. Calf thymus ss-DNA was coated and probed with the serum of C57BL/6 or Balb/c mice injected with PBS (*column 1*) and C57BL/6 mice injected with EL4 rafts or Balb/c mice injected with P3U1 rafts (*column 2*). The mean values of triplicate experiments are shown

immune responses against glycolipids in mice, a large amount of purified antigen usually must be immobilized by adsorbing it to the cell walls of bacteria, such as *Salmonella minnesota*, or by incorporating it into liposomes [12], whereas rafts themselves are insoluble and do not need to be immobilized. Furthermore, without mixing with Freund's adjuvant, rafts may retain adjuvant effects and be capable of inducing an immune response even in syngeneic mice.

It still remains unclear how monoglycolipid-specific antibodies are produced, which cells should be used for raft preparation, and to which glycolipids antibodies are predominantly produced. Although further experiments are certainly needed to answer these questions, raft immunization can be used as an effective method of producing monoclonal antibodies against glycolipids and can be applied as new approach in many fields.

Acknowledgments We thank Ms. S. Yamauchi for her excellent secretarial work. This work was supported in part by Health and Labour Sciences Research Grants and Grant for Child Health and Development from the Ministry of Health, Labour and Welfare of Japan, a grant from the Japan Health Sciences Foundation for Research on Health Sciences Focusing on Drug Innovation, JSPS. KAKENHI 18790263, the Budget for Nuclear Research of the Ministry of Education, Culture, Sports, Science and Technology, based on screening and counseling by the Atomic Energy Commission. This work was also supported by CREST, JST, and a grant from Charitable Trust Japan Leukemia Research Fund.

References

1. Katagiri, Y.U., Mori, T., Nakajima, H., Katagiri, C., Taguchi, T., Takeda, T., Kiyokawa, N., Fujimoto, J.: Activation of Src family kinase yes induced by Shiga toxin binding to globotriaosyl ceramide (Gb3/CD77) in low density, detergent-insoluble microdomains. J. Biol. Chem. **274**, 35278–35282 (1999)
2. Katagiri, Y.U., Ohmi, K., Katagiri, C., Sekino, T., Nakajima, H., Ebata, T., Kiyokawa, N., Fujimoto, J.: Prominent immunogenicity of monosialosyl galactosylgloboside, carrying a stage-specific embryonic antigen-4 (SSEA-4) epitope in the ACHN human renal tubular cell line—a simple method for producing monoclonal antibodies against detergent-insoluble microdomains/raft. Glycoconj. J. **18**, 347–353 (2001)
3. Asanuma, H., Takahashi, S., Ishikawa, M., Kamiguchi, K., Sato, N., Poppema, S., Fujimoto, J., Kikuchi, K.: A monoclonal antibody, 3G12, reacts with a novel surface molecule, Hal-1, with high expression in CD30-positive anaplastic large cell lymphomas. Br. J. Haematol. **106**, 55–63 (1999)
4. Katagiri, Y.U., Kiyokawa, N., Nakamura, K., Takenouchi, H., Taguchi, T., Okita, H., Umezawa, A., Fujimoto, J.: Laminin binding protein, 34/67 laminin receptor, carries stage-specific embryonic antigen-4 epitope defined by monoclonal antibody Raft.2. Biochem. Biophys. Res. Commun. **332**, 1004–1011 (2005)
5. Iizuka, J., Katagiri, Y., Tada, N., Murakami, M., Ikeda, T., Sato, M., Hirokawa, K., Okada, S., Hatano, M., Tokuhisa, T., Uede, T.: Introduction of an osteopontin gene confers the increase in B1 cell population and the production of anti-DNA autoantibodies. Lab. Invest. **78**, 1523–1533 (1998)
6. Jacob, F.: Mouse teratocarcinoma and embryonic antigens. Immunol. Rev. **33**, 3–32 (1977)
7. Tang, W.R., Kiyokawa, N., Eguchi, T., Matsui, J., Takenouchi, H., Honma, D., Yasue, H., Enosawa, S., Mimori, K., Itagaki, M., Taguchi, T., Katagiri, Y.U., Okita, H., Amemiya, H., Fujimoto, J.: Development of novel monoclonal antibody 4G8 against swine leukocyte antigen class I alpha chain. Hybridoma Hybridomics. **23**, 187–91 (2004)
8. Sawada, M., Moriya, S., Shinehara, R., Satomi, S., Miyagi, T.: Comparative study of sialidase activity and GM3 content in B16 melanoma variants with different metastatic potential. Acta. Biochim. Pol. **45**, 343–349 (1998)
9. Kawashima, I., Nakamura, O., Tai, T.: Antibody responses to gangliosides-series gangliosides in diffeent strains of inbred mice. Mol. Immunol. **29**, 625–632 (1992)
10. Yamazaki, Y., Nagatsuka, Y., Oshima, E., Suzuki, Y., Hirabayashi, Y., Hashikawa, T.: Comprehensive analysis of monoclonal antibodies against detergent-insoluble membrane/lipid rafts of HL60 cells. J. Immunol. Methods **311**, 106–116 (2006)
11. Stroud, M.R., Handa, K., Salyan, M.E., Ito, K., Levery, S.B., Hakomori, S., Reinhold, B.B., Reinhold, W.N.: Monosialogangliosides of human myelogenous leukemia HL60 cells and normal human leukocytes. 1. Separation of E-selectin binding from nonbinding gangliosides, and absence of sialosyl-Le(x) having tetraosyl to octaosyl core. Biochemistry **35**, 758–769 (1996)
12. Kannagi, R.: Monoclonal anti-glycosphingolipid antibodies. Methods Enzymol. **312**, 160–179 (2000)

Molecular Biology of the Cell
Vol. 18, 1586–1594, May 2007

Menstrual Blood-derived Cells Confer Human Dystrophin Expression in the Murine Model of Duchenne Muscular Dystrophy via Cell Fusion and Myogenic Transdifferentiation[D]

Chang-Hao Cui,*† Taro Uyama,* Kenji Miyado,* Masanori Terai,* Satoru Kyo,‡ Tohru Kiyono,§ and Akihiro Umezawa*

*Department of Reproductive Biology and Pathology, National Institute for Child Health and Development, Tokyo, 157-8535, Japan; †Department of Basic Medical Science, Mudanjiang Medical College, Mudanjiang, 157011, China; ‡Department of Obstetrics and Gynecology, Kanazawa University, School of Medicine, Kanazawa, 920-8640, Japan; and §Virology Division, National Cancer Center Research Institute, Tokyo, 104-0045, Japan

Submitted September 28, 2006; Revised January 19, 2007; Accepted February 6, 2007
Monitoring Editor: M. Bishr Omary

Duchenne muscular dystrophy (DMD), the most common lethal genetic disorder in children, is an X-linked recessive muscle disease characterized by the absence of dystrophin at the sarcolemma of muscle fibers. We examined a putative endometrial progenitor obtained from endometrial tissue samples to determine whether these cells repair muscular degeneration in a murine mdx model of DMD. Implanted cells conferred human dystrophin in degenerated muscle of immunodeficient mdx mice. We then examined menstrual blood–derived cells to determine whether primarily cultured nontransformed cells also repair dystrophied muscle. In vivo transfer of menstrual blood–derived cells into dystrophic muscles of immunodeficient mdx mice restored sarcolemmal expression of dystrophin. Labeling of implanted cells with enhanced green fluorescent protein and differential staining of human and murine nuclei suggest that human dystrophin expression is due to cell fusion between host myocytes and implanted cells. In vitro analysis revealed that endometrial progenitor cells and menstrual blood–derived cells can efficiently transdifferentiate into myoblasts/myocytes, fuse to C2C12 murine myoblasts by in vitro coculturing, and start to express dystrophin after fusion. These results demonstrate that the endometrial progenitor cells and menstrual blood–derived cells can transfer dystrophin into dystrophied myocytes through cell fusion and transdifferentiation in vitro and in vivo.

INTRODUCTION

Skeletal muscle consists predominantly of syncytial fibers with peripheral, postmitotic myonuclei, and its intrinsic repair potential in adulthood relies on the persistence of a resident reserve population of undifferentiated mononuclear cells, termed "satellite cells." In mature skeletal muscle, most satellite cells are quiescent and are activated in response to environmental cues, such as injury, to mediate postnatal muscle regeneration. After division, satellite cell progeny, termed myoblasts, undergo terminal differentiation and become incorporated into muscle fibers (Bischoff, 1994). Myogenesis is regulated by a family of myogenic transcription factors including MyoD, Myf5, myogenin, and MRF4 (Sabourin and Rudnicki, 2000). During embryonic development, MyoD and Myf5 are involved in the establishment of the skeletal muscle lineage (Rudnicki *et al.*, 1993), whereas myogenin is required for terminal differentiation (Hasty *et al.*, 1993; Nabeshima *et al.*, 1993). During muscle repair, satellite cells recapitulate the expression program of the myogenic genes manifested during embryonic development.

Dystrophin is associated with a large oligomeric complex of glycoproteins that provide linkage to the extracellular membrane (Ervasti and Campbell, 1991). In Duchenne muscular dystrophy (DMD), the absence of dystrophin results in destabilization of the extracellular membrane-sarcolemma-cytoskeleton architecture, making muscle fibers susceptible to contraction-associated mechanical stress and degeneration. In the first phase of the disease, new muscle fibers are formed by satellite cells. After depletion of the satellite cell pool in childhood, skeletal muscles degenerate progressively and irreversibly and are replaced by fibrotic tissue (Cossu and Mavilio, 2000). Like DMD patients, the mdx mouse lacks dystrophin in skeletal muscle fibers (Hoffman *et al.*, 1987; Sicinski *et al.*, 1989). However, the mdx mouse develops only a mild dystrophic phenotype, probably because muscle regeneration by satellite cells is efficient for most of the animal's life span (Cossu and Mavilio, 2000).

Myoblasts represent the natural first choice in cellular therapeutics for skeletal muscle because of their intrinsic myogenic commitment (Grounds *et al.*, 2002). However, myoblasts recovered from muscular biopsies are poorly expandable in vitro and rapidly undergo senescence (Cossu and Mavilio, 2000). An alternative source of muscle progenitor cells is therefore desirable. Cells with a myogenic potential are present in many tissues, and these cells readily

This article was published online ahead of print in *MBC in Press* (http://www.molbiolcell.org/cgi/doi/10.1091/mbc.E06-09-0872) on February 21, 2007.

[D] The online version of this article contains supplemental material at *MBC Online* (http://www.molbiolcell.org).

Address correspondence to: Akihiro Umezawa (umezawa@1985.jukuin.keio.ac.jp).

form skeletal muscle in culture (Gerhart *et al.*, 2001). We report here that human dystrophin expression in the mdx model of DMD is attributed to cell fusion of mdx myocytes with human menstrual blood–derived stromal cells.

MATERIALS AND METHODS

Isolation of Human Endometrial Cells from Menstrual Blood

Menstrual blood samples (n = 21) were collected in DMEM with antibiotics (final concentrations: 100 U/ml penicillin/streptomycin) and 2% fetal bovine serum (FBS), and processed within 24 h. Ethical approval for tissue collection was granted by the Institutional Review Board of the National Research Institute for Child Health and Development, Japan. The centrifuged pellets containing endometrium-derived cells were resuspended in high-glucose DMEM medium (10% FBS, penicillin/streptomycin), maintained at 37°C in a humidified atmosphere containing 5% CO_2, and allowed to attach for 48 h. Nonadherent cells were removed by changing the medium. When the culture reached subconfluence, the cells were harvested with 0.25% trypsin and 1 mM EDTA and plated to new dishes. After 2–3 passages, the attached endometrial stromal cells were devoid of blood cells. Human EM-E6/E7/hTERT-2 cells, endometrium-derived progenitors, were obtained from surgical endometrial tissue samples and were immortalized by E6, E7, and hTERT (Kyo *et al.*, 2003). C2C12 myoblast cells were supplied by RIKEN Cell Bank (The Institute of Physical and Chemical Research, Japan).

Flow Cytometric Analysis

Flow cytometric analysis was performed as previously described (Terai *et al.*, 2005). Cells were incubated with primary antibodies or isotype-matched control antibodies, followed by additional treatment with the immunofluorescent secondary antibodies. Cells were analyzed on an EPICS ALTRA analyzer (Beckman Coulter, Fullerton, CA). Antibodies against human CD13, CD14, CD29, CD31, CD34, CD44, CD45, CD50, CD54, CD55, CD59, CD73, CD90, CD105, CD117 (c-kit), CD133, HLA-ABC, and HLA-DR were purchased from Beckman Coulter, Immunotech (Marseille, France), Cytotech (Hellebaek, Denmark), and BD Biosciences PharMingen (San Diego, CA).

In Vitro Lentivirus-mediated Gene (EGFP) Transfer into EM-E6/E7/hTERT-2 Cells

Infection of EM-E6/E7/hTERT-2 cells with lentivirus having a CMV promoter and enhanced green fluorescent protein (EGFP) reporter resulted in high levels of EGFP expression in all cells. Cells were analyzed for EGFP expression by flow cytometry (Miyoshi *et al.*, 1997, 1998).

In Vitro Myogenesis

Menstrual blood–derived cells or EM-E6/E7/hTERT-2 cells were seeded onto collagen I–coated cell culture dishes (Biocoat, BD Biosciences, Bedford, MA) at a density of 1×10^4/ml in growth medium (DMEM, supplemented with 20% FBS). Forty-eight hours after seeding onto collagen I–coated dishes, cells were treated with 5-azacytidine for 24 h. Cell cultures were then washed twice with PBS and maintained in differentiation medium (DMEM, supplemented with either 2% horse serum (HS) or 1% insulin-transferrin-selenium supplement [ITS]). The differentiation medium was changed twice a week until the experiment was terminated.

RT-PCR Analysis of EM-E6/E7/hTERT-2 Cells and Menstrual Blood–derived Cells

Total RNA was prepared using Isogen (Nippon Gene, Tokyo, Japan). Human skeletal muscle RNA was purchased from TOYOBO (Osaka, Japan). RT-PCR of Myf5, MyoD, desmin, myogenin, myosin heavy chain-IIx/d (MyHC-IIx/d), and dystrophin was performed with 2 μg of total RNA. RNA for RT-PCR was converted to cDNA with a first-stand cDNA synthesis kit (Amersham Pharmacia Biotechnology, Piscataway, NJ) according to the manufacturer's recommendations. The sequences of PCR primers that amplify human but not mouse genes are listed in Supplementary Table 1. PCR was performed with TaKaRa recombinant Taq (Takara Shuzo, Kyoto, Japan) for 30 cycles, with each cycle consisting of 94°C for 30 s, 62°C or 65°C for 30 s, and 72°C for 20 s, with an additional 10-min incubation at 72°C after completion of the last cycle.

Immunohistochemical and Immunocytochemical Analysis

Immunohistochemical analysis was performed as previously described (Mori *et al.*, 2005). Briefly, the sections were incubated for 1 h at room temperature with mouse mAb against vimentin (Cone V9, DakoCytomation, Fort Collins, CO). After washing in PBS, sections were incubated with horseradish peroxidase-conjugated rabbit anti-mouse immunoglobulin, diluted, and washed in cold PBS. Staining was developed by using a solution containing diaminobenzidine and 0.01% H_2O_2 in 0.05 M Tris-HCl buffer, pH 6.7. Slides were counterstained with hematoxylin. In the cases of fluorescence, frozen sections fixed with 4% PFA were used. The antibodies against human dystrophin (NCL-DYS3; Novocastra, Newcastle upon Tyne, United Kingdom) or anti-human nuclei mouse mAb (clone 235-1, Chemicon, Temecula, CA) was used as a first antibody, and goat anti-mouse IgG conjugated with Alexa Fluor 488 or goat anti-mouse IgG antibody conjugated with Alexa Fluor 546 (Molecular Probes, Eugene, OR) was used as a second antibody.

Immunocytochemical analysis was performed as previously described (Mori *et al.*, 2005), with antibodies to skeletal myosin (Sigma, St. Louis, MO; product no. M 4276), MF20 (which reacts with all sarcomere myosin in striated muscles, Developmental Studies Hybridoma Bank, University of Iowa, IA), α-sarcomeric actin (Sigma, product no. A 7811), and desmin (Bio-Science Products, Emmenbruecke, Switzerland; no. 010031, clone: D9) in PBS containing 1% bovine serum albumin. As a methodological control, the primary antibody was omitted. In the cases of fluorescence, slides were incubated with Alexa Fluor 546–conjugated goat anti-mouse IgG antibody.

Western Blotting

Western blot analysis was performed as previously described (Mori *et al.*, 2005). Blots were incubated with primary antibodies (desmin, myogenin [Clone F5D, Santa Cruz Biotechnology], and dystrophin [NCL-DYSA, Novocastra]) for 1–2 h at room temperature. After washing three times in the blocking buffer, blots were incubated for 30 min with a horseradish peroxidase–conjugated secondary antibody (0.04 μg/ml) directed against the primary antibody. The blots were developed with enhanced chemiluminescence substrate according to the manufacturer's instructions.

Fusion Assay

EM-E6/E7/hTERT-2 cells (2500/cm^2) or EGFP-labeled EM-E6/E7/hTERT-2 cells (2500/cm^2) were cocultured with C2C12 myoblasts (2500/cm^2) for 2 d in DMEM supplemented with 10% FBS and then cultured for 7 additional days in DMEM with 2% HS to promote myotube formation. The cultures were fixed in 4% paraformaldehyde and stained with a mouse anti-human nuclei IgG1 mAb and the mouse anti-human dystrophin IgG2a mAb (or anti-myosin heavy chain IgG2b mAb MF-20). The cells were visualized with appropriate Alexa-fluor–conjugated goat anti-mouse IgG1 and IgG2a (or IgG2b) secondary antibodies (Molecular Probes). Total cell nuclei were stained with DAPI (4′,6-diamidino-2-phenylindole).

In Vivo Cell Implantation

Six- to 8-wk-old NOD/Shi-scid/IL-2 receptor −/− (NOG, CREA, Shizuoka, Japan) mice and 6- to 8-wk-old mdx-scid mice were implanted with EM-E6/E7/hTERT-2 cells and menstrual blood–derived cells in seven independent experiments. The cells (2×10^7) were suspended in PBS in a total volume of 100 μl and were directly injected into the right thigh muscle of NOG mice or mdx-scid mice. The mice were examined 3 wk after cell implantation, and the right thigh muscle was analyzed for human vimentin and dystrophin by immunohistochemistry. The antibodies to vimentin and dystrophin (NCL-DYS3) react with human vimentin and dystrophin-equivalent protein, but not murine protein.

RESULTS

Surface Marker Expression of Endometrium-derived Cells

We investigated myogenic differentiation of primary cells without gene introduction from menstrual blood, because menstrual blood on the first day of the period is considered to include endometrial tissue. We successfully cultured a large number of primary cells from menstrual blood. Menstrual blood–derived cells showed at least two morphologically different cell groups: small spindle-like cells and large stick-like cells, regarded as being passage day (PD) 1 or 2 (Figure 1, A and B, respectively). Surface markers of the menstrual blood–derived cells were evaluated by flow cytometric analysis. Surface markers of EM-E6/E7/hTERT-2 cells (Figure 1C) and menstrual blood–derived cells (Figure 1D) were evaluated by flow cytometric analysis (Figure 1E). In these experiments, the cells were cultured in the absence of any inductive stimuli. EM-E6/E7/hTERT-2 cells were positive for CD13, CD29 (integrin β1), CD44 (Pgp-1/ly24), CD54, CD55, CD59, CD73, and CD90 (Thy-1), implying that EM-E6/E7/hTERT-2 cells expressed mesenchymal cell–related antigens in our experimental setting. Menstrual blood–derived cells were positive for CD13, CD29, CD44, CD54, CD55, CD59, CD73, CD90, and CD105, implying that prolif-

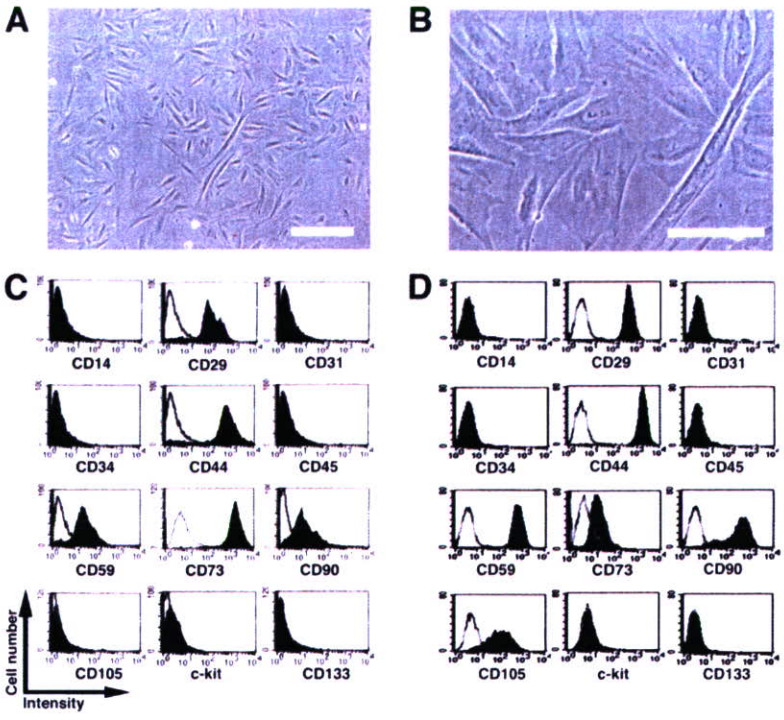

E

Surface marker	EM-E6/E7/ hTERT-2 cells	Menstrual blood cells	Surface marker	EM-E6/E7/ hTERT-2 cells	Menstrual blood cells
CD13	+	++	CD55	++	++
CD14	-	-	CD59	++	+++
CD29	++	+++	CD73	+++	+
CD31	-	-	CD90	++	+++
CD34	-	-	CD105	-	++
CD44	+++	+++	c-kit	-	-
CD45	-	-	CD133	-	-
CD50	-	-	HLA-ABC	++	++
CD54	+	++	HLA-DR	-	-

Figure 1. Surface marker expression of endometrium-derived cells. (A and B) Morphology of menstrual blood–derived cells, regarded as being PD 1 or 2. Scale bars, 200 μm (A), 100 μm (B). (C and D) Flow cytometric analysis of cell surface markers of EM-E6/E7/hTERT-2 cells (C) and menstrual blood–derived cells (D). (E) Further phenotypic analysis in EM-E6/E7/hTERT-2 cells and menstrual blood–derived cells are summarized. Peak intensity was estimated in comparison with isotype controls. +++, strongly positive (>100 times the isotype control); ++, moderately positive (<100 times but more than 10 times the isotype control); +, weakly positive (<10 times but more than twice the isotype control); −, negative (less than twice the isotype control).

erated and propagated cells express mesenchymal cell-related cell surface markers. Unlike EM-E6/E7/hTERT-2 cells, the menstrual blood–derived adherent cells were positive for CD105. EM-E6/E7/hTERT-2 cells and menstrual blood–derived cells expressed neither hematopoietic lineage markers, such as CD34, nor monocyte-macrophage antigens such as CD14 (a marker for macrophage and dendritic cells), or CD45 (leukocyte common antigen). The lack of expression of CD14, CD34, or CD45 suggests that EM-E6/E7/hTERT-2 cells and the menstrual blood–derived cell culture in the present study is depleted of hematopoietic cells. The cells were also negative for expression of CD31 (PECAM-1), CD50, c-kit, and CD133. The cell population was positive for HLA-ABC, but not for HLA-DR. These results demonstrate that almost all cells derived from endometrium are of mesenchymal origin or stromal origin.

Implanted Endometrium-derived Cells Induce De Novo Myogenesis in Immunodeficient NOG Mice

EM-E6/E7/hTERT-2 cells originate from the endometrial gland and are considered as endometrial progenitor cells or bipotential cells capable of differentiating into both glandular epithelial cells and endometrial stromal cells (Kyo *et al.*, 2003). To determine whether EM-E6/E7/hTERT-2 cells and menstrual blood–derived cells generate complete endometrial structure in vivo, like endometriosis, the cells without any treatment or induction were injected into the right thigh muscle of immunodeficient NOG mice. PBS without cells was injected into the left thigh muscles as a control. We failed to detect any endometrial structure in the cell-injected site. Immunohistochemical analysis using an antibody specific to human vimentin, an intermediate filament associated with a mesenchymal cell, revealed that the injected EM-E6/E7/hTERT-2 cells (Figure 2, A–F) or menstrual blood–derived cells (Figure 2, G–J) extensively migrated or infiltrated between muscular fibers (Figure 2, arrowheads). To investigate if the donor cells between muscular fibers occur as a result of cell migration, we performed a time-course analysis of implanted cells, as probed by human-specific antibody to vimentin (Supplementary Figure 1). Donor cells at 3 h after implantation are observed at the injection site, which is considered to be due to just injection of cells. Cells at 1–3 wk after implantation are detected between myocytes in the muscle bundle or muscular fascicle as well as in the interstitial tissue, implying that the donor cells between myotubes result from cell migration. Interestingly, some of the vimentin-positive implanted cells exhibited round-shaped structure (Figure 2, D, F, and J, arrows), suggesting that endometrium-derived cells are capable of differentiating into myoblasts/myotubes, and can contribute to skeletal muscle repair in patients suffering from genetic disorders such as DMD, similar to previous reports for marrow stromal cells (Dezawa *et al.*, 2005) and synovial membrane cells (De Bari *et al.*, 2003).

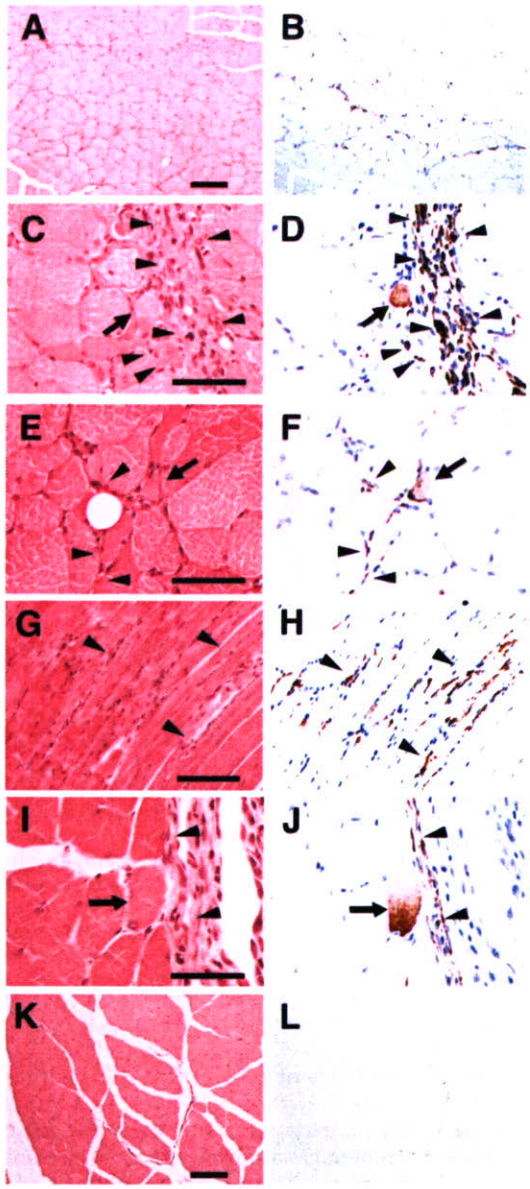

Figure 2. Implantation of endometrium-derived cells-derived cells into the muscle of NOG mice. EM-E6/E7/hTERT-2 cells (A–F) or menstrual blood–derived cells (G–J) cultured in absence of any stimuli were directly injected into the right thigh muscle of NOG mice. Immunohistochemical analysis was performed using antibody that reacts to human vimentin but not to murine vimentin. (A, C, E, G, I, and K) hematoxylin and eosin stain. (B, D, F, H, J, and L) immunohistochemistry. Note that vimentin-positive EM-E6/E7/hTERT-2 cells and menstrual blood–derived cells with a spindle morphology (C–J, arrowheads) extensively migrated into muscular bundles at 3 wk after injection, and some of the injected cells exhibited round structure (D, F, and J, arrows). Isotype mouse IgG1 served as a negative control (L). Scale bars, 100 μm (A, B, K, and L), 50 μm (C–F, I, and J), 90 μm (G and H).

Induction of Myogenic Differentiation in Endometrial Progenitor Cells In Vitro

EM-E6/E7/hTERT-2 cells at 2 wk (cultured in the DMEM supplemented with 20% FBS) after exposure to different concentrations (5, 10, and 100 μM) of 5-azacytidine were analyzed by immunostaining using anti-desmin antibody (Figure 3, A–E). The number of desmin-positive cells was significantly higher in experimental groups with 5 or 10 μM 5-azacytidine than in untreated control groups ($p < 0.05$) (Figure 3F). To investigate whether EM-E6/E7/hTERT-2 cells are capable of differentiating into skeletal muscle cells in vitro, the cells were exposed to 5 μM 5-azacytidine for 24 h and then subsequently cultured in the DMEM supplemented with 2% HS or serum-free ITS for up to 21 d. Skeletal myoblastic differentiation of the cells was analyzed by evaluating expression of MyoD, Myf5, desmin, myogenin, MyHC-IIx/d, and dystrophin by RT-PCR. The MyoD, desmin, myogenin, and dystrophin genes were constitutively expressed, but MyHC-IIx/d and Myf5 genes were not. The decline of MyoD was observed in both the 2% HS (Figure 3, G and H) and the serum-free ITS (Figure 3K). The expression of MyHC-IIx/d, as determined by RT-PCR and immunocytochemistry, significantly increased with 2% HS (Figure 3G) and serum-free ITS (Figure 3K). Immunocytochemical analysis indicated that α-sarcomeric actin (Figure 3I) and MyHC (Figure 3J) were detected in the cells incubated with 2% HS for 21 d.

In Vitro Myogenic Differentiation of Menstrual Blood-derived Cells

Menstrual blood–derived cells at 3 wk (cultured in DMEM supplemented with 20% FBS) after exposure to different concentrations (5, 10, and 100 μM) of 5-azacytidine were analyzed by immunostaining using anti-desmin antibody (data not shown). The number of desmin-positive cells was significantly higher in experimental groups with 5 or 10 μM 5-azacytidine than with 100 μM 5-azacytidine; for further in vitro experiments, the menstrual blood–derived cells were exposed to 5 μM 5-azacytidine for 24 h and then subsequently cultured in DMEM supplemented with low serum (2% HS) or serum-free ITS for up to 21 d (Figure 4). Myogenic potential of human menstrual blood–derived cells was analyzed by evaluating the expression of Myf5, MyoD, desmin, myogenin, MyHC-IIx/d, and dystrophin by RT-PCR. MyoD, desmin, and dystrophin genes were constitutively expressed in menstrual blood–derived cells, but MyHC-IIx/d and Myf5 were not (Figure 4A). For cells treated with 2% HS or serum-free ITS, the mRNA level of desmin and myogenin significantly increased after 3 d, and desmin steadily increased until day 21 (Figure 4, C and D). MyHC-IIx/d started to be expressed at a low level at day 21 of induction (Figure 4C). We then analyzed desmin expression by immunocytochemistry. Menstrual blood–derived cells were exposed to 5 μM 5-azacytidine for 24 h and then subsequently cultured in DMEM supplemented with 20% FBS for up to 2 wk. Desmin was readily detected in colonies of the menstrual blood–derived cells (Figure 4B). Western blot analysis indicated that desmin, myogenin, and dystrophin were highly expressed in the cells incubated for 3 wk (Figure 4, E–G). These results suggest that menstrual blood–derived cells are, like the EM-E6/E7/hTERT-2 cells, able to differentiate into skeletal muscle.

Regeneration of Dystrophin by Cell Implantation in the DMD Model mdx-scid Mouse

To investigate whether human EM-E6/E7/hTERT-2 cells and menstrual blood–derived cells can generate muscle tissue in vivo, cells without any treatment or induction were implanted directly into the right thigh muscles of mdx-scid mice (Supplementary Figure 2). The left thigh muscles were injected with PBS as an internal control. After 3 wk, myotubes in the muscle tissues injected with human EM-E6/E7/hTERT-2 cells and menstrual blood–derived cells expressed human dystrophin as a cluster (Figure 5, A, C, and D, EM-

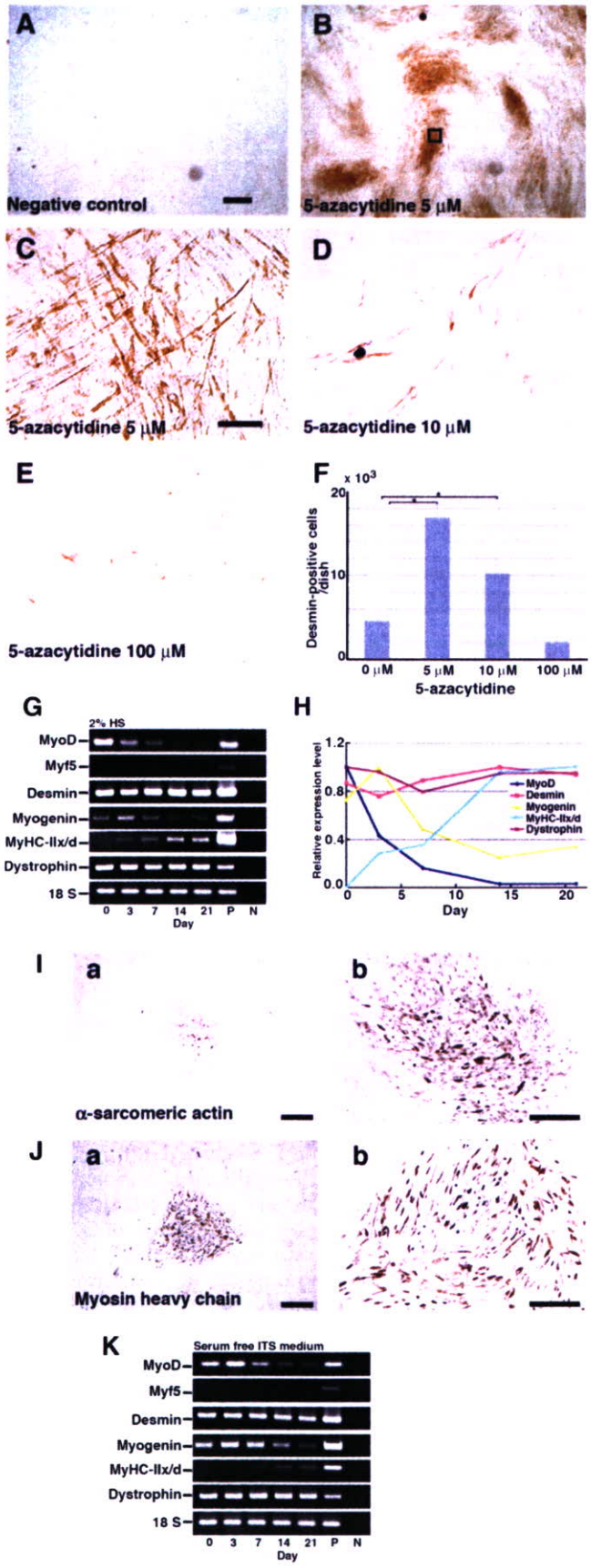

Figure 3. Expression of myogenic-specific genes during myogenic differentiation of EM-E6/E7/hTERT-2 cells. (A–E) Immunocytochemical analysis of EM-E6/E7/hTERT-2 cells using an antibody to desmin. (A) Omission of only the primary antibody to desmin serves as a negative control. (C) Higher magnification of inset in B. (F) Myogenic differentiation of EM-E6/E7/hTERT-2 cells with exposure to different concentrations (B, 5 μM; C, 5 μM; D, 10 μM; E, 100 μM) of 5-azacytidine. To estimate myogenic differentiation, the number of all the desmin-positive cells was counted for each dish (n = 3). Data were analyzed for statistical significance using ANOVA. EM-E6/E7/hTERT-2 cells were cultured in the DMEM supplemented with 2% HS, and serum-free ITS. (G and K) RT-PCR analysis with PCR primers allows amplification of the human MyoD, Myf5, desmin, myogenin, myosin heavy chain type IIx/d (MyHC-IIx/d), and dystrophin cDNA (from top to bottom). RNAs were isolated from EM-E6/E7/hTERT-2 cells at the indicated day after treatment with 5-azacytidine. RNAs from human muscle and H_2O served as positive (P) and negative (N) controls, respectively. Only the 18S PCR primer reacted with the human and murine cDNA. (H) Time course of MyoD, desmin, myogenin, MyHC-IIx/d, and dystrophin expression in the cells incubated with 2% HS for up to 21 d after 5-azacytidine treatment. Relative mRNA levels were determined using Multi Gauge Ver 2.0 (Fuji Film). The signal intensities of MyoD, desmin, and dystrophin mRNA at day 0, myogenin mRNA at day 3, and MyHC-II/d mRNA at day 21 were regarded as equal to 100%. (I and J) The cells were exposed to 5 μM 5-azacytidine for 24 h and then subsequently cultured in DMEM supplemented with 2% HS for 21 d. α-Sarcomeric actin (I) and skeletal myosin heavy chain (J) was detected by immunocytochemical analysis. Scale bars, 2 mm (A and B), 300 μm (C–E), 900 μm (Ia and Ja), 425 μm (Ib and Jb).

E6/E7/hTERT-2 cells, and 5B, menstrual blood–derived cells). Quantification analysis revealed that the percentage of dystrophin-positive myofibers after implantation of menstrual blood–derived cells was high, compared with that after implantation of EM-E6/E7/hTERT-2 cells (Figure 5E). Donor cells with EGFP fluorescence participated in myogenesis 3 wk after implantation (Supplementary Figure 3). EGFP-labeled EM-E6/E7/hTERT-2 cells became positive for human dystrophin (Figure 5C). Dystrophin was not detected in the muscle of mdx-scid mice and NOG mice without cell implantation because the antibody to dystrophin used in this study is human-specific, implying that dystrophin is transcribed from dystrophin genes of human donor cells but not from reversion of dystrophied myocytes in mdx-scid mice.

To determine if dystrophin expression in the donor cells is due to transdifferentiation or fusion, immunohistochemistry with an antibody against human nuclei (HuNucl) and DAPI stain was performed. If dystrophin expression is explained by fusion, dystrophin-positive myocytes must be demonstrated to have both human and murine nuclei. We examined almost all the 7-μm-thick serial histological sections parallel to the muscular bundle (longitudinal section) of the muscular tissues by confocal microscopy and found that dystrophin-positive myocytes have nuclei derived from both human and murine cells in the longitudinal section of the myocytes (Figure 5D), implying that dystrophin expression is attributed to fusion between murine host myocytes and human donor cells, rather than myogenic differentiation of EM-E6/E7/hTERT-2 cells and menstrual blood–derived cells per se.

Detection of Human Endometrial Cell Contribution to Myotubes in an In Vitro Myogenesis Model

To simulate in vivo phenomena, human endometrial cells were cocultured in vitro with murine C2C12 myoblasts for 2 d under proliferative conditions and then switched to differentiation conditions for an additional 7 d. Figure 6A provides an example of how human and mouse nuclei in the

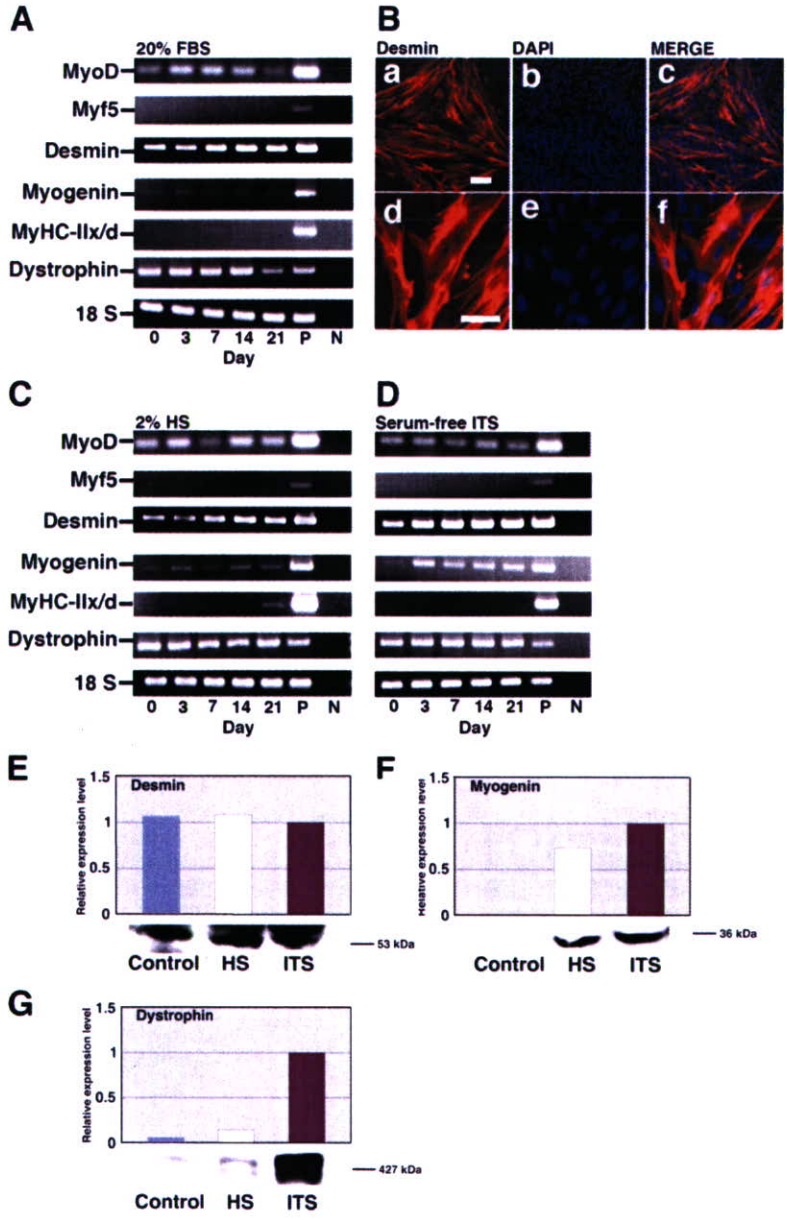

Figure 4. Expression of myogenic-specific genes in differentiated menstrual blood–derived cells. Menstrual blood–derived cells were cultured in DMEM supplemented with 20% FBS, 2% HS, or serum-free ITS medium. (A) RT-PCR analysis with PCR primers that allows amplification of the human MyoD, Myf5, desmin, myogenin, MyHC-IIx/d, and dystrophin cDNA (from top to bottom). RNAs were isolated from menstrual blood–derived cells in DMEM supplemented with 20% FBS at the indicated day after treatment with 5 μM 5-azacytidine for 24 h. RNAs from human muscle and H_2O served as positive (P) and negative (N) controls. Only the 18S PCR primer reacted with the human and murine cDNA. (B) Immunocytochemical analysis using an antibody to desmin (a–f) was performed on the menstrual blood–derived cells at 2 wk after exposure to 5 μM of 5-azacytidine for 24 h. The desmin-positive cells are shown at higher magnification (d–f). Merge of a and b is shown in c, and merge of d and e is shown in f. The images were obtained with a laser scanning confocal microscope. Scale bars, 200 μm (a–c) and 75 μm (d—f). (C and D) RT-PCR analysis of menstrual blood–derived cells on DMEM supplemented with 2% HS (C) or serum-free ITS medium (D) at the indicated day after exposure to 5 μM 5-azacytidine for 24 h. (E–G) Western blot analysis was performed on the cells cultured in myogenic medium indicated for 21 d. The blot was stained with desmin (E), myogenin (F), and dystrophin (G) antibodies followed by an HRP-conjugated secondary antibody.

EGFP-positive myotubes were detected. Multinucleated myotubes were revealed by the presence of specific human dystrophin (Figure 6, B and C) and myosin heavy chain (Figure 6D). Dystrophin was detected in cytoplasm in culture condition (Figure 6, B and C) despite evidence of cell surface localization in vivo. Human dystrophin and human nuclei were unequivocally identified by staining with antibodies to human dystrophin and human nuclei, whereas the numerous mouse nuclei present in this field, as shown by DAPI staining, are negative (Figure 6, B and C).

DISCUSSION

Skeletal muscle has a remarkable regenerative capacity in response to an extensive injury. Resident within adult skeletal muscle is a small population of myogenic precursor cells (or satellite cells) that are capable of multiple rounds of proliferation (estimated at 80–100 doublings), which are able to reestablish a quiescent pool of myogenic progenitor cells after each discrete regenerative episode (Mauro, 1961; Schultz and McCormick, 1994; Seale and Rudnicki, 2000; Hawke and Garry, 2001). Although muscle regeneration is a highly efficient and reproducible process, it ultimately is exhausted, as observed in senescent skeletal muscle or in patients with muscular dystrophy (Gussoni *et al.*, 1997; Cossu and Mavilio, 2000). In the present study, we investigated the myogenic potential of human endometrial tissue-derived immortalized EM-E6/E7/TERT-2 cells and primary cells derived from human menstrual blood. Human menstrual blood–derived cells proliferated over at least 25 PDs (9 passages) for more than 60 d and stopped dividing before 30 PDs. This cessation of cell division is probably due to replicative senescence or shortening of telomere length. Cell life span of menstrual blood cells is relatively short when compared with human fetal cells (Imai *et al.*, 1994; Terai *et al.*, 2005), and this shorter cell life span may be attributed to shorter telomere length of adult cells (i.e., endometrial stromal cells) at the start of cell cultivation, as is the case with hematopoietic stem cells (Suda *et al.*, 1984).

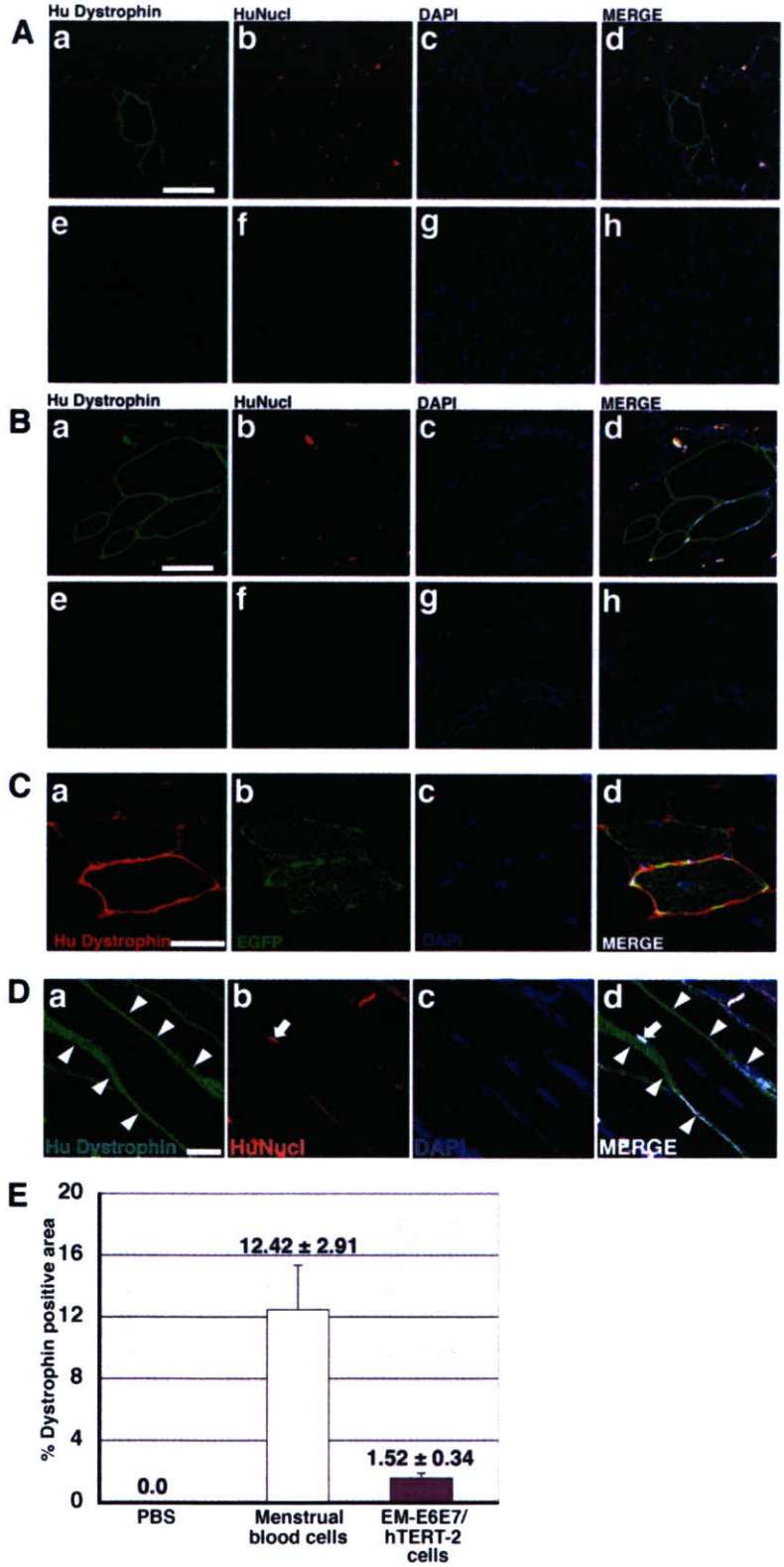

Figure 5. Conferral of dystrophin to mdx myocytes by human endometrial cells. (A and B) Immunohistochemistry analysis using an antibody against human dystrophin molecule (green), human nuclei (HuNucl, red), and DAPI staining (blue) on thigh muscle sections of mdx-scid mice after direct injection of EM-E6/E7/hTERT-2 cells (A) or menstrual blood–derived cells (B) without any treatment or induction. (C) EGFP-labeled EM-E6/E7/hTERT-2 cells without any treatment or induction were directly injected into the thigh muscle of mdx-scid mice. Immunohistochemistry revealed the incorporation of implanted cells into newly formed EGFP-positive myofibers, which expressed human dystrophin 3 wk after implantation. (A and B) As a methodological control, the primary antibody to dystrophin was omitted (e and f). (D) Immunohistochemistry analysis using an antibody against human dystrophin molecule (green, arrowheads), human nuclei (HuNucl, red, arrow), and DAPI staining (blue) on thigh muscle sections of mdx-scid mice after direct injection of human EM-E6/E7/hTERT-2 cells without any treatment or induction. (A and B) Merge of a–c is shown in d, and merge of e–g is shown in h. (C and D) Merge of a–c is shown in d. Scale bars, 50 μm (A and B), 20 μm (C and D). (E) Quantitative analysis of human dystrophin-positive myotubes. Menstrual blood–derived cells or EM-E6/E7/hTERT-2 cells without any treatment or induction were directly injected into thigh muscle of mdx-scid mice. The percentage of human dystrophin–positive-myofiber areas was calculated 3 wk after implantation of the EM-E6/E7/hTERT-2 cells or menstrual blood–derived cells. Injection of PBS without cells into mdx-scid myofibers was used as a control.

Menstrual blood–derived cells had a high replicative ability similar to progenitors or stem cells that display a long-term self-renewal capacity and had a much higher growth rate in our experimental conditions than marrow-derived stromal cells (Mori *et al.*, 2005). In addition, the myogenic potential of menstrual blood–derived cells, i.e., a high frequency of desmin-positive cells after induction, is much greater than expected. The higher myogenic differentiation ratio can be explained just by alteration of cell characteristics from epithelial and mesenchymal bipotential cells or heterogeneous populations of cells to cells with the mesenchymal phenotype in our cultivation condition, as determined by

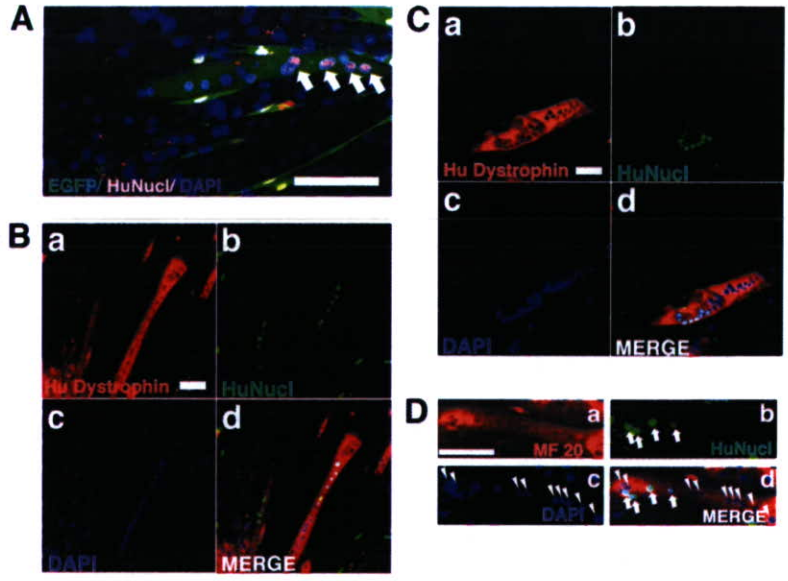

Figure 6. Detection of human endometrial cell contribution to myotubes in an in vitro myogenesis model. EGFP-labeled EM-E6/E7/hTERT-2 cells (A) or EM-E6/E7/hTERT-2 cells (B) or menstrual blood–derived cells (C and D) were cocultured with C2C12 myoblasts for 2 d under conditions that favored proliferation. The cultures were then changed to differentiation media for 7 d to induce myogenic fusion. (A) Myotubes were revealed by EGFP (green); human nuclei were detected by antibody specific to human nuclei (HuNucl, red, arrows). (B–D) Myotubes were revealed by specific human dystrophin mAb NCL-DYS3 (B and C, red) or anti-myosin heavy chain mAb MF-20 (D, red). (D) Human nuclei were detected by antibody specific to human nuclei (HuNucl, green, arrows). Total cell nuclei in the culture were stained with DAPI (blue, arrowheads). (B–D) Merge of a–c are shown in d. The cultures were then changed to differentiation media for 7 d to induce myogenic fusion. Scale bars, 100 μm (A–D).

cell surface markers (Figure 1, C–E). MyoD-positive cells are present in many fetal chick organs such as brain, lung, intestine, kidney, spleen, heart, and liver (Gerhart *et al.*, 2001), and these cells can differentiate into skeletal muscle in culture. Constitutive expression of MyoD, desmin, and myogenin, all markers for skeletal myogenic differentiation in both immortalized EM-E6/E7/hTERT-2 cells and menstrual blood–derived cells, implies either that most of these cells are myogenic progenitors or that these cells have myogenic potential. Expression of MyoD, one of the basic helix-loop-helix transcription factors that directly regulate myocyte cell specification and differentiation (Edmondson and Olson, 1993), occurs at the early stage of myogenic differentiation, whereas myogenin is expressed later, related to cell fusion and differentiation (Aurade *et al.*, 1994).

Acquisition or recovery of dystrophin expression in dystrophic muscle is attributed to two different mechanisms: 1) myogenic differentiation of implanted or transplanted cells and 2) cell fusion of implanted or transplanted cells with host muscle cells. Recovery of dystrophin-positive cells is explained by muscular differentiation of implanted marrow stromal cells and adipocytes (Dezawa *et al.*, 2005; Rodriguez *et al.*, 2005). In contrast, implantation of normal myoblasts into dystrophin-deficient muscle can create a reservoir of normal myoblasts that are capable of fusing with dystrophic muscle fibers and restoring dystrophin (Mendell *et al.*, 1995; Terada *et al.*, 2002; Wang *et al.*, 2003; Dezawa *et al.*, 2005; Rodriguez *et al.*, 2005). In this study using menstrual blood–derived cells, our findings—that the implantation of immortalized EM-E6/E7/hTERT-2 cells and menstrual blood–derived cells improved the efficiency of muscle regeneration and dystrophin delivery to dystrophic muscle in mice—is explained by both possibilities or the latter possibility alone, because cells expressing human dystrophin had both murine and human nuclei, located in the center and periphery of dystrophic muscular fiber, respectively (Figures 5D, in vivo, and 6, A–D, in vitro).

DMD is a devastating X-linked muscle disease characterized by progressive muscle weakness attributable to a lack of dystrophin expression at the sarcolemma of muscle fibers (Mendell *et al.*, 1995; Rodriguez *et al.*, 2005), and there are no effective therapeutic approaches for muscular dystrophy at present. Human menstrual blood–derived cells are obtained by a simple, safe, and painless procedure and can be expanded efficiently in vitro. In contrast, isolation of mesenchymal stem cells/mesenchymal cells from other sources, such as bone marrow and adipose tissue, is accompanied by a painful and complicated operation. Efficient fusion systems of our immortalized human EM-E6/E7/hTERT-2 cells and menstrual blood–derived cells with host dystrophic myocytes may contribute substantially to a major advance toward eventual cell-based therapies for muscle injury or chronic muscular disease. Finally, we would like to reemphasize that human menstrual blood–derived cells possess high self-renewal capacity, whereas biopsied myoblasts capable of differentiating into muscular cells are poorly expandable in vitro and rapidly undergo senescence (Cossu and Mavilio, 2000).

ACKNOWLEDGMENTS

We express our sincere thanks to J. Hata for support throughout this work, to H. Abe for providing expert technical assistance, to K. Saito for secretarial work, and to A. Crump for reviewing the manuscript. This study was supported by grants from the Ministry of Education, Culture, Sports, Science, and Technology (MEXT) of Japan; the Ministry of Health, Labor, and Welfare Sciences Research Grants; by a research grant on Health Science focusing on Drug Innovation from the Japan Health Science Foundation; by the program for promotion of Fundamental Studies in Health Science of the Pharmaceuticals and Medical Devices Agency; by a research grant for Cardiovascular Disease from the ministry of Health, Labor, and Welfare; and by a grant for Child Health and Development from the Ministry of Health, Labor, and Welfare.

REFERENCES

Aurade, F., Pinset, C., Chafey, P., Gros, F., and Montarras, D. (1994). Myf5, MyoD, myogenin and MRF4 myogenic derivatives of the embryonic mesenchymal cell line C3H10T1/2 exhibit the same adult muscle phenotype. Differentiation *55*, 185–192.

Bischoff, R. (1994). The satellite cell and muscle regeneration. In: Myology: Basic and Clinical, ed. A. Engel, C. Franzini-Armstrong, and D. A. Fischman, New York: McGraw-Hill, Health Professions Division, 97–118.

Cossu, G., and Mavilio, F. (2000). Myogenic stem cells for the therapy of primary myopathies: wishful thinking or therapeutic perspective? J. Clin. Invest. *105*, 1669–1674.

De Bari, C., Dell'Accio, F., Vandenabeele, F., Vermeesch, J. R., Raymackers, J. M., and Luyten, F. P. (2003). Skeletal muscle repair by adult human mesenchymal stem cells from synovial membrane. J. Cell Biol. *160*, 909–918.

Dezawa, M., Ishikawa, H., Itokazu, Y., Yoshihara, T., Hoshino, M., Takeda, S., Ide, C., and Nabeshima, Y. (2005). Bone marrow stromal cells generate muscle cells and repair muscle degeneration. Science *309*, 314–317.

Edmondson, D. G., and Olson, E. N. (1993). Helix-loop-helix proteins as regulators of muscle-specific transcription. J. Biol. Chem. *268*, 755–758.

Ervasti, J. M., and Campbell, K. P. (1991). Membrane organization of the dystrophin-glycoprotein complex. Cell *66*, 1121–1131.

Gerhart, J., Bast, B., Neely, C., Iem, S., Amegbe, P., Niewenhuis, R., Miklasz, S., Cheng, P. F., and George-Weinstein, M. (2001). MyoD-positive myoblasts are present in mature fetal organs lacking skeletal muscle. J. Cell Biol. *155*, 381–392.

Grounds, M. D., White, J. D., Rosenthal, N., and Bogoyevitch, M. A. (2002). The role of stem cells in skeletal and cardiac muscle repair. J. Histochem. Cytochem. *50*, 589–610.

Gussoni, E., Blau, H. M., and Kunkel, L. M. (1997). The fate of individual myoblasts after transplantation into muscles of DMD patients. Nat. Med. *3*, 970–977.

Hasty, P., Bradley, A., Morris, J. H., Edmondson, D. G., Venuti, J. M., Olson, E. N., and Klein, W. H. (1993). Muscle deficiency and neonatal death in mice with a targeted mutation in the myogenin gene. Nature *364*, 501–506.

Hawke, T. J., and Garry, D. J. (2001). Myogenic satellite cells: physiology to molecular biology. J. Appl. Physiol. *91*, 534–551.

Hoffman, E. P., Brown, R. H., Jr., and Kunkel, L. M. (1987). Dystrophin: the protein product of the Duchenne muscular dystrophy locus. Cell *51*, 919–928.

Imai, S., Fujino, T., Nishibayashi, S., Manabe, T., and Takano, T. (1994). Immortalization-susceptible elements and their binding factors mediate rejuvenation of regulation of the type I collagenase gene in simian virus 40 large T antigen-transformed immortal human fibroblasts. Mol. Cell. Biol. *14*, 7182–7194.

Kyo, S., Nakamura, M., Kiyono, T., Maida, Y., Kanaya, T., Tanaka, M., Yatabe, N., and Inoue, M. (2003). Successful immortalization of endometrial glandular cells with normal structural and functional characteristics. Am. J. Pathol. *163*, 2259–2269.

Mauro, A. (1961). Satellite cell of skeletal muscle fibers. J. Biophys. Biochem. Cytol. *9*, 493–495.

Mendell, J. R. *et al.* (1995). Myoblast transfer in the treatment of Duchenne's muscular dystrophy. N. Engl. J. Med. *333*, 832–838.

Miyoshi, H., Blomer, U., Takahashi, M., Gage, F. H., and Verma, I. M. (1998). Development of a self-inactivating lentivirus vector. J. Virol. *72*, 8150–8157.

Miyoshi, H., Takahashi, M., Gage, F. H., and Verma, I. M. (1997). Stable and efficient gene transfer into the retina using an HIV-based lentiviral vector. Proc. Natl. Acad. Sci. USA *94*, 10319–10323.

Mori, T. *et al.* (2005). Combination of hTERT and bmi-1, E6, or E7 induces prolongation of the life span of bone marrow stromal cells from an elderly donor without affecting their neurogenic potential. Mol. Cell. Biol. *25*, 5183–5195.

Nabeshima, Y., Hanaoka, K., Hayasaka, M., Esumi, E., Li, S., Nonaka, I., and Nabeshima, Y. (1993). Myogenin gene disruption results in perinatal lethality because of severe muscle defect. Nature *364*, 532–535.

Rodriguez, A. M. *et al.* (2005). Transplantation of a multipotent cell population from human adipose tissue induces dystrophin expression in the immunocompetent mdx mouse. J. Exp. Med. *201*, 1397–1405.

Rudnicki, M. A., Schnegelsberg, P. N., Stead, R. H., Braun, T., Arnold, H. H., and Jaenisch, R. (1993). MyoD or Myf-5 is required for the formation of skeletal muscle. Cell *75*, 1351–1359.

Sabourin, L. A., and Rudnicki, M. A. (2000). The molecular regulation of myogenesis. Clin. Genet. *57*, 16–25.

Schultz, E., and McCormick, K. M. (1994). Skeletal muscle satellite cells. Rev. Physiol. Biochem. Pharmacol. *123*, 213–257.

Seale, P., and Rudnicki, M. A. (2000). A new look at the origin, function, and "stem-cell" status of muscle satellite cells. Dev. Biol. *218*, 115–124.

Sicinski, P., Geng, Y., Ryder-Cook, A. S., Barnard, E. A., Darlison, M. G., and Barnard, P. J. (1989). The molecular basis of muscular dystrophy in the mdx mouse: a point mutation. Science *244*, 1578–1580.

Suda, J., Suda, T., and Ogawa, M. (1984). Analysis of differentiation of mouse hemopoietic stem cells in culture by sequential replating of paired progenitors. Blood *64*, 393–399.

Terada, N., Hamazaki, T., Oka, M., Hoki, M., Mastalerz, D. M., Nakano, Y., Meyer, E. M., Morel, L., Petersen, B. E., and Scott, E. W. (2002). Bone marrow cells adopt the phenotype of other cells by spontaneous cell fusion. Nature *416*, 542–545.

Terai, M., Uyama, T., Sugiki, T., Li, X. K., Umezawa, A., and Kiyono, T. (2005). Immortalization of human fetal cells: the life span of umbilical cord blood-derived cells can be prolonged without manipulating p16INK4a/RB braking pathway. Mol. Biol. Cell *16*, 1491–1499.

Wang, X., Willenbring, H., Akkari, Y., Torimaru, Y., Foster, M., Al-Dhalimy, M., Lagasse, E., Finegold, M., Olson, S., and Grompe, M. (2003). Cell fusion is the principal source of bone-marrow-derived hepatocytes. Nature *422*, 897–901.

STEM CELLS
TISSUE-SPECIFIC STEM CELLS

The Significant Cardiomyogenic Potential of Human Umbilical Cord Blood-Derived Mesenchymal Stem Cells In Vitro

NOBUHIRO NISHIYAMA,[a] SHUNICHIRO MIYOSHI,[a,b] NAOKO HIDA,[a,c] TARO UYAMA,[c] KAZUMA OKAMOTO,[d] YUKINORI IKEGAMI,[a] KENJI MIYADO,[c] KAORU SEGAWA,[f] MASANORI TERAI,[c] MICHIIE SAKAMOTO,[e] SATOSHI OGAWA,[a] AKIHIRO UMEZAWA[c]

[a]Cardiopulmonary Division, Keio University School of Medicine, Tokyo, Japan; [b]Keio University School of Medicine, Institute for Advanced Cardiac Therapeutics, Tokyo, Japan; [c]Department of Reproductive Biology and Pathology, National Research Institute for Child Health and Development, Tokyo, Japan; [d]Department of Surgery, [e]Department of Pathology, and [f]Department of Microbiology and Immunology, Keio University School of Medicine, Tokyo, Japan

Key Words. Physiology • Transplantation • Action potentials • Cells • Heart failure

ABSTRACT

We tested the cardiomyogenic potential of the human umbilical cord blood-derived mesenchymal stem cells (UCBMSCs). Both the number and function of stem cells may be depressed in senile patients with severe coronary risk factors. Therefore, stem cells obtained from such patients may not function well. For this reason, UCBMSCs are potentially a new cell source for stem cell-based therapy, since such cells can be obtained from younger populations and are being routinely utilized for clinical patients. The human UCBMSCs (5×10^3 per cm^2) were cocultured with fetal murine cardiomyocytes ([CM] 1×10^5 per cm^2). On day 5 of coculitivation, approximately half of the green fluorescent protein (GFP)-labeled UCBMSCs contracted rhythmically and synchronously, suggesting the presence of electrical communication between the UCBMSCs. The fractional shortening of the contracted UCBMSCs was 6.5% ± 0.7% (n = 20). The UCBMSC-derived cardiomyocytes stained positive for cardiac troponin-I (clear striation +) and connexin 43 (diffuse dot-like staining at the margin of the cell) by the immunocytochemical method. Cardiac troponin-I positive cardiomyocytes accounted for 45% ± 3% of GFP-labeled UCBMSCs. The cardiomyocyte-specific long action potential duration (186 ± 12 milliseconds) was recorded with a glass microelectrode from the GFP-labeled UCBMSCs. CM were observed in UCBMSCs, which were cocultivated in the same dish with mouse cardiomyocytes separated by a collagen membrane. Cell fusion, therefore, was not a major cause of CM in the UCBMSCs. Approximately half of the human UCBMSCs were successfully transdifferentiated into cardiomyocytes in vitro. UCBMSCs can be a promising cellular source for cardiac stem cell-based therapy. STEM CELLS *2007;25:2017–2024*

Disclosure of potential conflicts of interest is found at the end of this article.

INTRODUCTION

Autologous stem cells are believed to be a potential cellular source for stem cell-based therapy, since they have the ability to proliferate and differentiate into cardiomyocytes [1–4]. Many types of cells, such as embryonic stem cells [5, 6], myoblasts [7, 8], bone marrow hematopoietic cells [9, 10], and mesenchymal stem cells (MSCs) [11–13], have been transplanted to restore damaged heart function in animal models. Autologous mononuclear cells [14–17] and myoblasts [18] have been injected into ischemic hearts clinically to improve impaired cardiac function. Despite the dramatic improvement of cardiac function by the stem-cell-based therapy in the animal model [10, 19], only modest effects were observed in the clinical study [14–17, 20]. One of the reasons for this may have been the extremely low rate of cardiomyogenesis of the stem cells in vitro and in vivo [2, 13, 21]. Therefore, the improvement of cardiac function may have been due to grafted stem cell-induced neovascularization [13, 22] and/or the paracrine effect [23]. Another reason may have been the ages and disease histories of the patients. Recent papers have shown that the number and function of the circulating stem cells were depressed in older patients and in patients with diabetes mellitus [24, 25], suggesting that stem cells obtained from patients with coronary risk factors may not function well. This suggests limits to the utilization of autologous stem cells for the ischemic cardiomyopathy patient. On the other hand, in order to do allogenic stem cell transplantation, human leukocyte antigen (HLA)-type matching is very important for the stable survival of grafts. Therefore, the sample, which can be noninvasively collected from many volunteers, is a desirable source of stem cells due to the ease of establishing cell banks that can store all HLA-types.

Recently, umbilical cord blood (UCB) banking for transplantation of hematopoietic stem cells has become popular [26]. If we can utilize UCB for heart failure patients, we can utilize this UCB stem cell bank network system immediately. UCB-derived stem cells may be superior to marrow-derived stem cells because they are obtained from infants. UCB contains circulating stem/progenitor cells, and the cells contained in UCB are

Correspondence: Shunichiro Miyoshi, M.D., Ph.D., Cardiopulmonary Division of Keio University School of Medicine, 35-Shinanomachi Shinjuku-ku, Tokyo 160-8582, Japan. Telephone: +81-3-3353-1211 (ext. 62310); Fax: +81-3-3353-2502; e-mail: smiyoshi@cpnet.med.keio.ac.jp Received October 23, 2006; accepted for publication May 6, 2007; first published online in STEM CELLS *EXPRESS* May 10, 2007. 1066-5099/2007/$30.00/0 doi: 10.1634/stemcells.2006-0662

known to be quite distinct from those contained in bone marrow and adult peripheral blood [27]. UCB transplantation has been reported to improve cardiac function [28–30]. That study, however, used a fraction of hematopoietic lineage and failed to show any clear evidence for cardiomyogenesis in vivo. In the present study, we focus on the mesenchymal lineage of UCB.

Isolation, characterization, and differentiation of clonally expanded umbilical cord blood-derived mesenchymal stem cells (UCBMSCs) have been reported [31, 32]. UCBMSCs have been found to have multipotency, and the immunophenotype of the clonally expanded cells is consistent with that reported for bone marrow mesenchymal stem cells [33, 34]. Kim et al. [35] showed modest but significant functional recovery of impaired cardiac function by transplantation of human unrestricted somatic stem cells obtained from umbilical cord blood that expressed mesenchymal cell surface markers [34]; therefore, mesenchymal lineage of the cells obtained from UCB may have potential therapeutic advantage in cardiac stem cell therapy. However, in vitro [33] and in vivo [34, 35], cardiomyogenic transdifferentiation ability have not yet been extensively studied. In the present study, we find that UCBMSCs have a strong potential for cardiomyogenic transdifferentiation.

MATERIALS AND METHODS

Isolation and Cell Culture of UCBMSCs

The detailed isolation method has been described previously [33]. A few colonies were found in the culture dish bottom 1 month after the collected cells were cultured in Dulbecco's modified Eagle's medium (DMEM) with 10% fetal bovine serum (FBS). One colony was trypsinized using a colony cylinder and then used for the experiment. We designated the monoclonal cell line as UCBMSC. The cells were prepared for infection with recombinant retroviruses expressing the human telomerase reverse transcriptase (TERT), as described previously [2, 33]. Stably transduced cells with an expanded life span were designated UCBMSC-TERT. The cells were cultured for further experiments under the approval of the Ethics Committee of our institute.

Preparation of Murine Fetal Cardiomyocytes

Fetal cardiomyocytes were obtained from the hearts of day 17 mouse fetuses [2]. Hearts were minced with scissors and washed with phosphate-buffered saline (PBS), and the minced hearts were incubated in PBS with 0.05% trypsin and 0.25 mM EDTA (ethylenediamine-*N*,*N*,*N*′,*N*′-tetraacetic acid) (Invitrogen, Carlsbad, CA, http://www.invitrogen.com) for 10 minutes at 37°C. After DMEM supplemented with 10% FBS was added, the cardiomyocytes were centrifuged at 1,000 rpm for 5 minutes. The pellet was then resuspended in 10 ml of DMEM with 10% FBS and incubated on glass dishes for 1 hour to separate the cardiomyocytes from fibroblasts. The floating cardiomyocytes were collected and replated at 1×10^5 per cm^2.

Coculture System of UCBMSCs/UCBMSCs-TERT and Murine Fetal Cardiomyocytes

We employed a coculture system with fetal cardiomyocytes to induce cardiac transdifferentiation, since in vitro simulation of the heart by the environment has been shown to be an efficient means of inducing the transdifferentiation of human marrow-derived MSC [2]. Cryopreserved UCBMSCs and UCBMSCs-TERT were used for the experiment. After thawing, the cells were cultured for at least two passages to stabilize the condition of the cell before the cardiomyogenic induction. UCBMSCs and UCBMSCs-TERT were labeled with enhanced green fluorescent protein (GFP) by recombinant adenovirus transfection as described previously [2]. These cells were then exposed to 3 μM 5-azacytidine (5-azaC; Sigma-Aldrich, St. Louis, http://www.sigmaaldrich.com) for 24 hours to induce cell transdifferentiation or were left untreated. Then, 5×10^3 per cm^2 of the cells were plated on the murine cardiomyocyte. The images were stored using a digital video system. The cell contraction was analyzed using a homemade image edge detection program made using Igor Pro 4 (WaveMetrics Inc., Portland, OR, http://www.wavemetrics.com). We administered 10 μM caffeine, 10 μM verapamil, or 1 μM thapsigargin to observe contraction of differentiated UCBMSCs.

Immunocytochemistry

A laser confocal microscope (FV1000; Olympus, Tokyo, http://www.olympus-global.com) was used for immunocytochemical analysis. The UCBMSCs and UCBMSCs-TERT were stained with mouse monoclonal anti-human cardiac troponin-I antibody (number 4T21 Lot 98/10-T21-C2; HyTest, Turku, Finland, http://www.hytest.fi) diluted 1:300, monoclonal anti-α actinin antibody (Sigma) diluted 1:300, or anti-connexin 43 antibody (Sigma) diluted 1:300. Nuclei were stained with 4′-6-diamidino-2-phenylindole (Wako Chemical, Osaka, Japan, http://www.wako-chem.co.jp/english) at 1:300. tetramethylrhodamine iso-thiocyanate (TRITC)-conjugated goat anti-mouse IgG (Sigma), TRITC-conjugated goat anti-rabbit IgG (Sigma), and Cy5-conjugated goat anti-mouse IgG (Chemicon, Temecula, CA, http://www.chemicon.com) were used as secondary antibodies.

Calculation of Induction Rate

After 1 week, UCBMSCs and UCBMSCs-TERT cultivated with or without murine fetal cardiomyocytes were detached from the dish by 0.1% trypsin and 0.25 mM EDTA for 5 minutes. The mass of cells obtained was then dissociated by 0.5% collagenase type-II (Worthington Biochemical, Lakewood, NJ, http://www.worthington-biochem.com) and 10 mM 2,3-butanedione monoxime (Sigma)-containing culture medium for 20–60 minutes. The isolated cells were seeded on poly-L-lysine coated dishes and stained. A confocal laser microscope was used to examine the cells. The cardiomyogenic induction rate was calculated as the fraction of human cardiac troponin-I-positive cells in the GFP-positive cells. The rate was calculated as the average from more than 10 separate experiments.

Examination of Chromosomes of UCBMSCs and Murine Cell Chimeras

Chromosomes from UCBMSCs cocultivated with murine cardiomyocyte for 1 week were stained by using a human chromosome-specific probe and a mouse chromosome-specific probe (Chromosome Science Labo, Hokkaido, Japan) and spectral karyotyping with fluorescence in situ hybridization (FISH) chromosome painting technique (Spectral Imaging, Vista, CA, http://www.spectral-imaging.com), according to the manufacturer's protocol.

Coculture of UCBMSCs-TERT and Murine Fetal Cardiomyocytes Separated by a Collagen Membrane

UCBMSCs-TERT and murine fetal cardiomyocytes were cocultured separately within the same dish. The murine fetal cardiomyocytes were seeded on top of a floating collagen film (CM-6; Koken, Tokyo, http://www.kokenmpc.co.jp/english), and the UCBMSCs-TERT were seeded on the bottom of the film. These two types of cells were, therefore, separated by a high-density atelocollagen film with a thickness of 30–40 μm, as shown in Figure 5E, that is permeable only for small molecules, less than 5,000 molecular weight (MW). After 1 week of cocultivation, the cells were analyzed immunocytochemically.

RNA Extraction and Reverse Transcriptase-Polymerase Chain Reaction

Total RNA was extracted from the UCBMSCs and UCBMSCs-TERT with RNeasy (Qiagen, Hilden, Germany, http://www1.qiagen.com). Human cardiac RNA was purchased (Clontech, Palo Alto, CA, http://www.clontech.com). RNA for reverse transcription-polymerase chain reaction (RT-PCR) was converted to cDNA with a first-strand cDNA synthesis kit (GE Healthcare, Bucking-

hamshire, U.K., http://www.gehealthcare.com) according to the manufacturer's recommendations. RT-PCR was performed by using primers for the following genes: Csx/Nkx-2.5, GATA4; cardiac hormones: human atrial natriuretic peptide (hANP), human brain natriuretic peptide (hBNP); cardiac structural proteins: cardiac troponin-I, cardiac troponin T, myosin heavy chain (MHC), myosin light chain-2a (MLC2a), cardiac-actin; ion channel: hyperpolarization-activated cyclic nucleotide-gated potassium channel 2 (HCN2); and 18s rRNA (18s rRNA was used as an internal control). PCR primers were prepared such that they would amplify the human but not the mouse genes [2] (supplemental online Table 1).

Flow Cytometric Analysis

Cells were detached and stained for 30 minutes at 4°C with primary antibodies and immunofluorescent secondary antibodies. After washing, the cells were analyzed using a FACScan (BD Biosciences, San Diego, http://www.bdbiosciences.com), and the data were analyzed with the CellQuest software (BD Sciences). Antibodies (anti-human CD13, CD14, CD24, CD29, CD31, CD34, CD44, CD45, CD54, CD55, CD59, CDw90, CD105, CD117, CD133, CD140a, CD157, CD164, CD166, Flk-1, SSEA-1, SSEA-3, and SSEA-4) were purchased from Beckman Coulter (Fullerton, CA, http://www.beckmancoulter.com), Immunotech (Luminy, France, http://www.beckmancoulter.com/products/pr_immunology.asp), Cytotech (Hellebaek, Denmark, http://www.cytotech.dk), Santa Cruz Biotechnology Inc. (Santa Cruz, CA, http://www.scbt.com), RDI (Concord, MA http://www.researchd.com), and Pharmingen Pharmaceutical Co. (San Diego).

Electrophysiological Experiment

Action potentials (APs) from the spontaneously beating GFP-positive UCBMSCs and UCBMSCs-TERT were recorded by use of standard microelectrodes, as described previously [2]. After the APs of the targeted cells were recorded, the dye (Alexa 568) was injected by electrophoresis (−5 nA for 10–20 seconds) to confirm the recorded APs obtained from GFP-positive cells. The extent of dye transfer was monitored under a fluorescent microscope.

RESULTS

Cardiomyogenic Transdifferentiation of UCBMSCs and UCBMSCs-TERT

On day 3 after starting the cocultivation, a few GFP-positive UCBMSCs and UCBMSCs-TERT started to contract (n = 68). On day 7, the beating of the murine cardiomyocytes stopped, whereas approximately half of the GFP-positive UCBMSCs and UCBMSCs-TERT beat strongly in a synchronized manner.

Immunocytochemistry revealed that a significant number of UCBMSCs and UCBMSCs-TERT expressing GFP were stained positive by the anti-human cardiac troponin-I antibody (Fig. 1A–1E, supplemental online Fig. 1A–1H). A clear striation pattern of cardiac troponin-I staining of UCBMSCs can be observed in higher magnification view (Fig. 1). Interestingly, troponin-I staining and GFP were observed alternately in a striated manner, suggesting that the troponin-I was expressed in the GFP-positive cells (Fig. 1 E). Clear striations were observed with red fluorescence of α-actinin in the differentiated UCBMSCs and UCBMSCs-TERT (Fig. 2B, 2H). Arrays of cardiomyocytes can be frequently observed (Fig. 2H). Connexin 43 staining (Fig. 2C, 2I) showed a clear and diffuse pattern around the margin of each GFP-positive cardiomyocyte, suggesting that these human transdifferentiated cardiomyocytes have tight electrical coupling with each other.

We also calculated the percentage of the human cardiac troponin-I-positive cells to determine the cardiomyogenic transdifferentiation rate of UCBMSCs and UCBMSCs-TERT. Since there was no essential difference between the UCBMSCs and UCBMSCs-TERT, calculated data from both cell types are averaged and shown in Figure 3. Although UCBMSCs without cocultivation did not show any troponin-I expression (Fig. 3H, 3K), 45% ± 3% of UCBMSCs became positive for human cardiac troponin-I antibody as a result of the cocultivation (Fig.

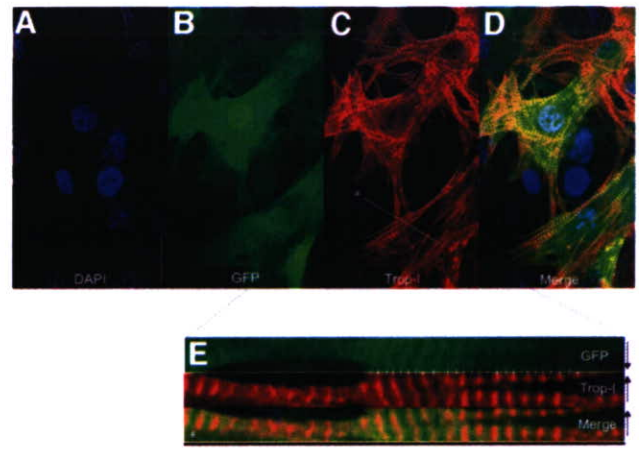

Figure 1. Cardiomyogenic transdifferentiation of umbilical cord blood mesenchymal stem cells. Laser confocal microscopic view of immunocytochemistry of differentiated umbilical cord blood mesenchymal stem cells with anti-cardiac troponin-I antibody. Superimposed images (Merge) of **(A–C)** are shown in **(D)**. Significant numbers of differentiated GFP-positive umbilical cord blood-derived mesenchymal stem cells (green) had troponin-I (red) in their cytoplasm (yellow as a result of "merging" **[D]**). Nuclei are stained with DAPI **([A]**, blue). Clear troponin-I (red) staining with striation pattern can be observed. GFP **([B]**, green) and Trop-I **([C]**, red) along the white line in **(C)** are magnified in panel **(E)**. Interestingly, troponin-I staining and GFP were observed alternately in a striated manner, suggesting the troponin-I expressed in the GFP-positive cells. Scale bars in the figure denote 20 μm. Abbreviations: DAPI, 4,6-diamidino-2-phenylindole; GFP, green fluorescent protein; Trop-I, troponin-I.

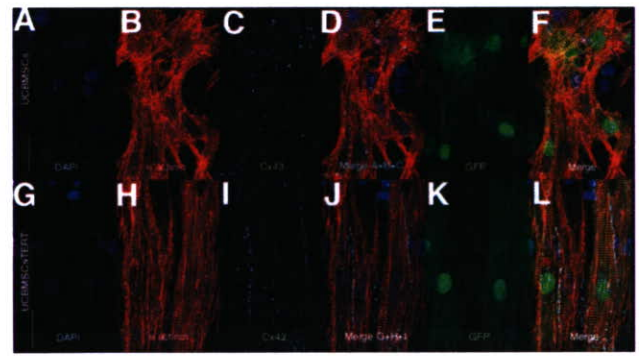

Figure 2. Immunocytochemical analysis of umbilical cord blood mesenchymal stem cell stained with anti-sarcomeric α-actinin and connexin 43. Laser confocal microscopic view of immunocytochemistry of differentiated umbilical cord blood mesenchymal stem cells and cells transduced with human TERT gene to prolong their life span (UCBMSCs-TERT) with anti-sarcomeric α-actinin **([B, H]**; α-actinin, red) and connexin 43 **([C, I]**; Cx43, cyan) antibody. Superimposed images (Merge) of **(A–C)** and **(G–I)** are shown in **(D)** and **(J)**, respectively. Clear striation pattern of α-actinin and diffuse Cx43 dot-like staining around the margin of the UCBMSCs were observed. These cells are GFP-positive UCBMSCs **([E, K]**; GFP, green. Merged images of **[D, E]** and **[J, K]** are **[F]** and **[L]**, respectively). Nuclei are stained with DAPI **([A, G]**, blue). It is noted that arrays of the UCBMSC-derived cardiomyocytes are sometimes observed **(J)**. Scale bars in the figure denote 50 μm. Abbreviations: DAPI, 4,6-diamidino-2-phenylindole; GFP, green fluorescent protein; UCBMSCs, umbilical cord blood mesenchymal stem cells; UCBMSCs-TERT, umbilical cord blood mesenchymal stem cells-telomerase reverse transcriptase.

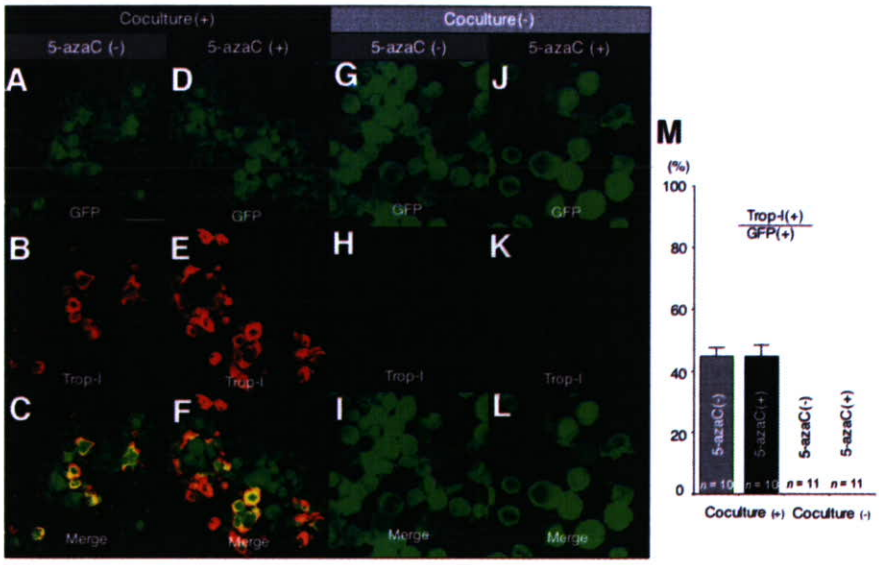

Figure 3. Calculation of cardiomyogenic transdifferentiation ratio of umbilical cord blood mesenchymal stem cells (UCBMSCs). **(A–L):** Representative laser confocal image of cardiac troponin-I **([B, E, H, K]**; Trop-I, red) staining to calculate cardiomyogenic transdifferentiation rate of UCBMSCs. Upper bar denotes the culture conditions for each panel presented bellow. (Coculture; cocultivation with fetal murine cardiomyocyte, 5-azaC; pretreatment with 5-azacytidine.) Approximately half of the isolated GFP-positive UCBMSCs **([A, D]**; GFP, green) stained positive for Trop-I **(B, E)** as a result of coculture. A superimposed image of **(A)** + **(B)** and **(D)** + **(E)** are shown in **(C)** and **(F)**, respectively. On the other hand, UCBMSCs **(G, J)** do not show any Trop-I staining **(H, K)**. Scale bars in the figure denote 50 μm. The cardiomyogenic transdifferentiation rate of UCBMSCs was defined as the percentage of Trop-I-positive cells in the GFP-positive cells. Measured data were averaged and are shown **(M)**. Error bars denote SEM (n = 20). Abbreviations: 5-azaC, 5-azacytidine; GFP, green fluorescent protein; Trop-I, troponin-I.

3B, 3E). It is noted that cardiomyogenic transdifferentiation could be observed in the cocultivated UCBMSCs and UCBMSCs-TERT without any 5-azaC pretreatment.

Cell Fusion-Independent Cardiomyogenic Transdifferentiation

Cell fusion has been shown to be quite a rare phenomenon [4, 36]; however, it may contribute to the generation of cardiomyocytes in our system. Nuclear fusion between the cocultivated UCBMSCs-TERT and fetal murine cardiomyocytes was observed in only approximately 0.09% (2/2165) of the cocultivated cells by FISH analysis (Fig. 4A–4D). In the differentiated cardiomyocyte, there is no cell having double nuclei in the isolated GFP-positive UCBMSCs. Furthermore, in cocultures of UCBMSCs-TERT with fetal murine cardiomyocytes separated by a collagen membrane (Fig. 4E), we observed beating GFP-positive cells and human cardiac troponin-I expression (Fig. 4F–4L) (n = 8). Because these two cell types were not attached directly to each other, it was concluded that the cardiomyogenesis in the present study was mainly caused by the transdifferentiation of the UCBMSCs.

Expression of Cardiomyocyte-Specific Genes and Surface Markers of UCBMSCs and UCBMSCs-TERT

We analyzed the cocultured UCBMSCs and UCBMSCs-TERT in terms of gene expression and by immunocytochemistry and electrical recording. RT-PCR was performed with primers that hybridized with human cardiomyocyte-specific genes but not with the murine orthologues (second column from the right, Fig. 5A). Differentiated UCBMSCs-TERT expressed Csx/Nkx-2.5, GATA4, hANP, hBNP, cardiac-actin, MHC, MLC2a, cardiac troponin T, cardiac troponin-I, and HCN2. Interestingly, all of the analyzed genes except for the MHC and MLC2a were expressed in UCBMSCs and UCBMSCs-TERT before the induction, implying that UCBMSCs may have cardiomyogenic potential as a default state, like CMG cells, in which Csx/Nkx-2.5 and GATA4 are constitutively expressed before induction [3]. Sequence analysis revealed that the sequences of the cDNAs matched those of the human genes.

Surface markers of the UCBMSCs-TERT were evaluated by flow cytometric analysis. The results showed that all of the

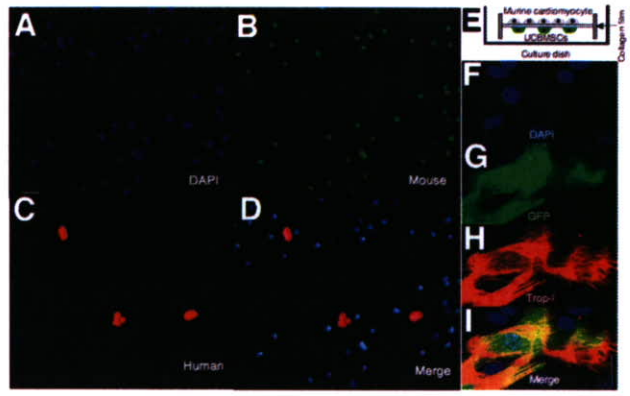

Figure 4. Cell fusion-independent cardiomyogenesis in UCBMSCs. **(A–D):** Representative images of fluorescent in situ hybridization for human nucleus and mouse nucleus are shown. Nuclei are stained with DAPI **([A]**; blue). Mouse nuclei were detected as green **(B)** and human nuclei were detected as red **(C)**. Superimposed image of **(A–C)** is shown in **(D)** (Merge). See text for details. **(E):** The experimental scheme is shown. The murine cardiomyocytes and UCBMSCs were cocultured on the top and the bottom of a collagen membrane, respectively. The cocultivated UCBMSCs and murine cardiomyocytes were separated by the 50-μm-thick collagen membrane. Nuclei were stained with DAPI **([F]**, blue) and UCBMSCs were labeled with GFP **([G]**, green). UCBMSCs were stained with anti-human cardiac troponin-I antibody **([H]**, red), and the merged images (DAPI, GFP, Trop-I) are shown **(I)**. Scale bars in the figure denote 20 μm. Abbreviations: DAPI, 4,6-diamidino-2-phenylindole; GFP, green fluorescent protein; Trop-I, troponin-I; UCBMSCs, umbilical cord blood mesenchymal stem cells.

UCBMSCs-TERT were positive for CD29 (integrin β1), CD44 (Pgp-1/Iy-24), CD54, CD55, CD59, CDw90, CD105, CD157, CD164, CD166, and SSEA-4 and negative for CD14 (a marker for macrophage and dendritic cells), CD31 (platelet endothelial cell adhesion molecule-1), CD34, CD45 (leukocyte common antigen), CD117 (c-kit), CD133, CD140a, Flk-1, SSEA-1, and SSEA-3 (Fig. 5B). Our UCBMSCs are negative for CD34, CD45, Flk-1, and CD133, thus differing from hematopoietic stem cell and from circulating endothelial progenitor cells. It is noted that our UCBMSCs are weakly positive for SSEA4 [37], an embryonic stem cell marker. Thus, UCBMSCs may be more plastic for transdifferentiation than other somatic stem cells.

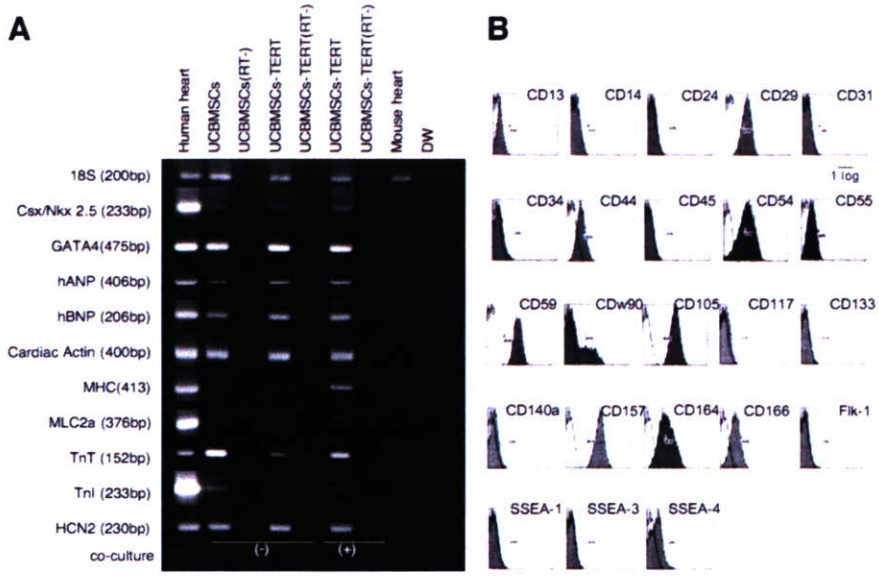

Figure 5. Expression of cardiomyocyte-specific genes in UCBMSCs and cell surface markers of UCBMSCs. **(A):** Expression of cardiomyocyte-specific genes in UCBMSCs and UCBMSCs-TERT. Reverse transcription-polymerase chain reaction (PCR) was performed with PCR primers with specificity for human genes encoding cardiac proteins but not for the corresponding murine genes. Only the 18S PCR primer used as a positive control reacted with both the human and murine genes. Human heart and mouse heart were used as a positive control and negative control, respectively. Almost all human cardiac genes were constitutively expressed in the default state. **(B):** Flow cytometric analysis of UCBMSCs with fluorescein isothiocyanate-coupled antibodies against the human surface antigens. Abbreviations: DW, distilled water; hANP, human atrial natriuretic peptide; hBNP, human brain natriuretic peptide; HCN2, hyperpolarization-activated cyclic nucleotide-gated potassium channel 2; MHC, myosin heavy chain; MLC2a, myosin light chain-2a; RT, reverse transcriptase; TnI, cardiac troponin I; TnT, cardiac troponin T; UCBMSCs, umbilical cord blood mesenchymal stem cells; UCBMSCs-TERT, umbilical cord blood mesenchymal stem cells-telomerase reverse transcriptase.

Functional Analysis of Differentiated UCBMSCs and UCBMSCs-TERT In Vitro

APs were recorded from spontaneously beating GFP-positive UCBMSCs and UCBMSCs-TERT. Alexa 568 was injected into cells via a recording microelectrode to stain the cells and confirm that the APs were generated by GFP-positive UCBMSCs (Fig. 6A, 6C). Since the dye did not diffuse into the murine cardiomyocytes, there were no tight cell-to-cell heterologous connections, that is, gap junctions. In most experiments, Alexa 568 diffused into the GFP-positive adjacent UCBMSCs and UCBMSCs-TERT, suggesting that homologous cell-to-cell connections had been established within 1 week after the start of cocultivation. The APs obtained from UCBMSCs and UCBMSCs-TERT showed clear cardiomyocyte-specific sustained plateaus. It was, therefore, concluded that they were the APs of cardiomyocytes, not of smooth muscle, nerve cells, or skeletal muscle (Fig. 6B, 6D). The measured parameters of the recorded APs were averaged (Fig. 6E). UCBMSCs and UCBMSCs-TERT did not have a marked pacemaker potential and had the character of working cardiomyocytes or ordinary cardiomyocytes. The rhythm of almost all of the UCBMSCs and UCBMSCs-TERT had become regular at 1 week. The fractional shortening (% FS) of the UCBMSCs and UCBMSCs-TERT was analyzed (Fig. 6F–6I) using a cell edge detection program. The GFP-positive cells contracted simultaneously within the whole visual field, suggesting tight electrical communication. There was no difference of % FS between the UCBMSCs and UCBMSCs-TERT. The % FS was augmented significantly by the administration of caffeine and inhibited by the administration of verapamil or thapsigargin (Fig. 7).

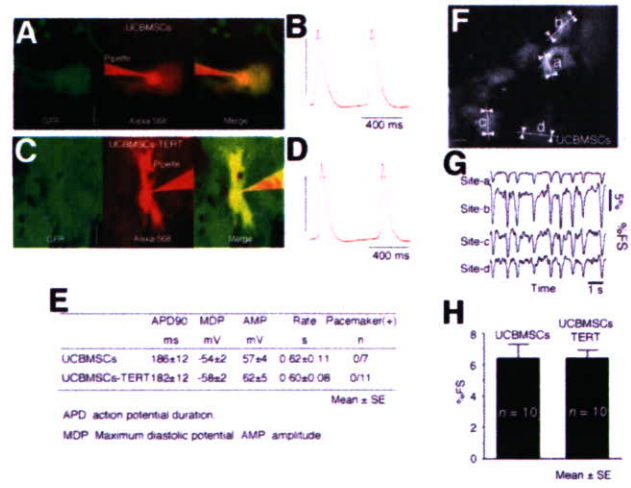

Figure 6. Functional analysis of UCBMSCs and UCBMSCs-TERT. Representative fluorescent microscopic images during action potential (AP) recording are shown **(A, C)**. Immediately after the AP recordings, alexa568 dye (red) was injected into the cell via the same recording electrode to confirm that the recorded AP was obtained from GFP-positive UCBMSCs. **(B, D):** Representative APs obtained from **(A)** and **(C)** respectively. The dotted line denotes the 0 mV level and the vertical line denotes 50 mV. **(E):** The measured AP parameters were averaged and are shown. **(F):** A representative still image from cell motion analysis is shown. The white arrowheads point to the automatically detected cell edge. The detected fractional shortening along the white line obtained from site-a, -b, -c, -d **(G)**. **(H):** The measured % FS was averaged and is shown. Abbreviations: AMP, amplitude; APD, action potential duration; % FS, fractional shortening; GFP, green fluorescent protein; MDP, maximum diastolic potential; ms, milliseconds; s, second; UCBMSCs, umbilical cord blood mesenchymal stem cells; UCBMSCs-TERT, umbilical cord blood mesenchymal stem cells-telomerase reverse transcriptase.

DISCUSSION

Physiologically Functioning Cardiomyocytes Can Be Generated from UCBMSCs In Vitro

Compared with the cardiomyogenic differentiation efficiency of the marrow-derived MSC (0.3%) [2], a significant number of the UCBMSCs transdifferentiated into cardiomyocytes in vitro in the present study. Generated cardiomyocytes showed physiologically functioning ability, that is, cardiomyocyte-specific

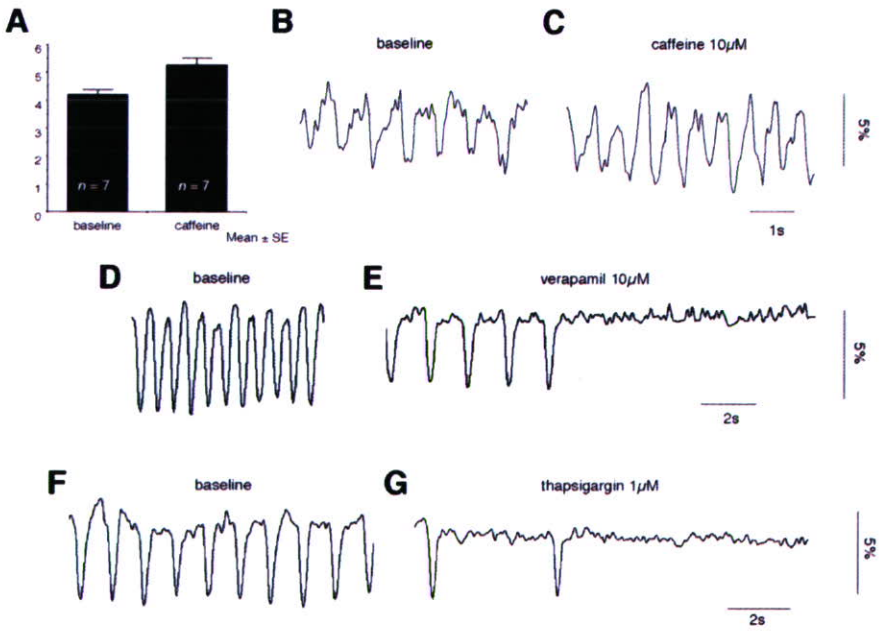

Figure 7. The effect of the drug administration on contraction of differentiated umbilical cord blood mesenchymal stem cells (UCBMSCs). The detected fractional shortening (% FS) of the differentiated UCBMSCs before and after the administration of caffeine **(A–C)**, verapamil **(D, E)**, and thapsigargin **(F, G)** are shown. The caffeine slightly increased the beating rate and increased the % FS significantly **(A)**. On the other hand, immediately after the administration of verapamil **(D)** or thapsigargin **(F)**, the beating rate decreased, then ceased **(E, G)**. Abbreviation: s, second.

APs with long duration (more than 100 milliseconds) and spontaneous contraction. The fact that each UCBMSC beats in a synchronized manner and the fact of the diffuse connexin 43 staining together suggest the formation of tight electrical coupling among the UCBMSCs. In our previous paper, we used the cells immediately after being quickly thawed from cryopreserved UCBMSCs, then failed to observe cardiomyogenic transdifferentiation in the small number of observations [33]. Recently, however, we felt at least two passages should be required to stabilize and regain cardiomyogenic transdifferentiation ability in UCBMSCs and our several cell lines.

Highly Cardiomyogenic Differentiation Potential

In the marrow-derived stem cell, mesenchymal lineage has a cardiomyogenic transdifferentiation potential [2, 3]; hematopoietic cell lineage does not [21]. This implies that mesenchymal lineage of the cell in UCB might have the ability to transdifferentiate into cardiomyocytes. Several in vivo experiments using UCB have shown feasible effects in restoring cardiac function in the myocardial infarction model [28–30]. However, these experiments used CD34+ or CD133+ hematopoietic lineage of the cell in UCB and failed to show any clear evidence of cardiomyogenesis. Surface marker analysis revealed UCBMSCs as differing from hematopoietic stem cells and from circulating endothelial progenitor cells. Kögler et al. [34] reported that stem cells obtained from UCB, so-called unrestricted somatic stem cells (USSCs), have a pluripotent differential potential with a similar surface marker pattern, that is, negative for CD34 and CD45 and positive for CD29 and CD44, that is typical for mesenchymal cells. Furthermore, Kim et al. [35] showed that USSCs improved impaired cardiac function in vivo. Although the two papers showed modest evidence for cardiomyogenic potential of USSCs in vivo, experiments had not been extensively done to show the evidence of cardiac transdifferentiation. Finally, these papers failed to show clear evidence for cell fusion-independent cardiomyogenesis and efficiency of cardiomyogenic differentiation. In the present study, we show significant potential of cell fusion-independent cardiomyogenesis of UCBMSCs.

Comparisons with Other Stem Cells for Cardiology

Cardiac precursor cells (CPCs) [38] should be a promising stem cell source for cardiac regeneration therapy. However, CPCs failed to differentiate to the physiologically functioning cardiomyocyte in vitro, and cardiomyogenic differentiation efficiency in vivo was 29%–40%. Thus, cardiomyogenic differentiation efficiency might not be so markedly high compared with the UCBMSCs. Moreover, it is very difficult to match the donor-recipient HLA-type, and there is still a longstanding ethical problem. An embryonic stem cell is a pluripotential stem cell that has a cardiomyogenic differentiation potential. But there are still critical underlying problems, that is, teratoma formation [39], genomic alteration in long-term culture [40], and the ethical problem. Differing from embryonic stem cells, our RT-PCR data suggest constitutive expression of Nkx2.5/Csx and GATA4 and other cardiac structure mRNA with the ability of self-renewal. This suggests that some population of the UCBMSCs has cardiomyogenic potential as the default state, and they may be termed cardiac precursor cells in light of their biological features. Recently, we reported that human endometrial gland-derived mesenchymal cells also have a high cardiomyogenic potential [41]. This suggests that they may be a stem cell source for heart disease. However, for male patients, there is no choice for autologous transplantation of this cell and no running stem cell bank for this cell. On the other hand, if UCBMSCs were isolated and frozen at the time of birth, they could later be thawed for use by the donor who required cardiac stem cell therapy at a later age. Furthermore, UCB banking has played a major role for hematopoietic stem cell transplantation for leukemia treatment. If we utilize a world-wide UCB bank system for cardiac stem cell therapy, we may be able to utilize UCBMSCs for cardiac stem cell therapy in the near future. Since several reports showed that mesenchymal cells cause immunological tolerance [42–44], we speculate that only a minimum administration of immunosuppressive agents may be sufficient to control rejection of the allogenic UCBMSC transplantation, if we match the other MHC antigen by utilizing the stem cell bank system.